BORYANA KRASIMIROVA TSENKOVA

SYNTHESIS AND CHARACTERIZATION OF IONIC CO-CRYSTALS OF ENANTIOPURE AND RACEMIC PROLINE

UNIVERSIDADE DO ALGARVE
FACULDADE DE CIÊNCIAS E TECNOLOGIA
2017

BORYANA KRASIMIROVA TSENKOVA

SYNTHESIS AND CHARACTERIZATION OF IONIC CO-CRYSTALS OF ENANTIOPURE AND RACEMIC PROLINE

Erasmus Mundus MSc in Chemical Innovation and Regulation
Mestrado Erasmus Mundus em Inovação Química e Regulamentação

Trabalho efetuado sob a orientação de:

Work supervised by:

Prof. Fabrizia Grepioni (University of Bologna)

Prof. Teresa Duarte (Centro de Química Estrutural)

UNIVERSIDADE DO ALGARVE
FACULDADE DE CIÊNCIAS E TECNOLOGIA
2017

SYNTHESIS AND CHARACTERIZATION OF IONIC CO-CRYSTALS OF ENANTIOPURE AND RACEMIC PROLINE

Declaration of Authorship

I declare that I am the author of this work, which is original. The work cites other authors and works, which are adequately referred in the text and are listed in the bibliography.

Boryana Krasimirova Tsenkova

ACKNOWLEDGEMENTS

I am grateful to the European Commission for the scholarship funded within the Erasmus+ KA1 Programme ref.2013-0241-Erasmus Master Joint Master Degree in Chemical Innovation and Regulation.

I would like to express my gratitude for the wonderful collaboration between UAlg, CQE and UniBo, which allowed me to perform all the experimental work under the supervision of **Prof. Fabrizia Grepioni (UniBo)** and **Prof. Teresa Duarte (CQE).** I would like to express my heartfelt gratitude to both of them for their support, expert guidance, understanding and continuous encouragement throughout this project.

This thesis would not have been possible without the support of the members of the Crystal Engineering groups at University of Bologna and CQE. I would like to express my gratitude for their kind guidance and assistance to **Lorenzo degli Esposti**, **Oleksii Shemchuk**, **Dr. Vânia Andre**, **Prof. Lucia Maini** and **Dr. Katia Rubini**. It has been a great honor to work in the research group of **Prof. Dario Braga.**

I would like to express my deepest appreciation to – **Prof. Isabel Cavaco** and **Prof. Emilio Tagliavini** for creating and coordinating this programme.

Finally, I would like to thank my parents, my sister, and my partner, for providing me with unconditional love and emotional support through this challenging project. I would like to thank my ChIR family for creating a supportive and academically stimulating environment.

ABSTRACT

An ionic co-crystal (ICC) is a multicomponent solid formed by at least an organic molecule and an inorganic salt in a defined stoichiometric ratio. ICCs have the potential to alter physicochemical properties (such as solubility and thermal stability) of a pure organic material of interest, and recent research has also highlighted the possibility of chiral resolution through ICC formation.

The purpose of the current work was to synthesize and characterize novel ionic co-crystals of racemic proline with lithium halides using mechanochemical and solution techniques, and to investigate the solid-state chiral resolution ability of lithium. The synthesis of molecular and ionic co-crystals of enantiopure and racemic proline with different inorganic salts and organic co-formers was attempted in order to obtain novel compounds with modified properties. Powder and Single Crystal X-ray diffraction, TGA and DSC were the main techniques used for the characterization of the novel compounds.

The results obtained confirm the potential for chiral resolution through ICC formation as conglomerate and racemate ICCs were obtained. In the racemate ICCs, at least in the 1:1 stoichiometry amino acid to lithium halide, a very consistent pattern was observed - the homochiral preference of Lithium resulted in the formation of homochiral columns. Previously described in the literature ICC of $(DL\text{-}Proline)_2 \bullet ZnCl_2$ with homochiral columns spiked our interest and a different synthesis procedure was followed, resulting in the formation of a $(DL\text{-}Proline)_2 \bullet ZnCl_2$ polymorph without the homochiral columns. These results encourage further studying the factors that promote homochiral column formation in the crystal packing - a possible precursor to conglomerate formation. Narrowing down these factors could allow us in the future to fine-tune the co-crystallization of chiral compounds as a conglomerate or a racemate ICC and pave the road towards novel methods for chiral resolution.

Keywords: ionic co-crystal, chiral resolution, proline, conglomerate

RESUMO

Co-cristal iónico (CCI) é um sólido multicomponente formado por pelo menos uma molécula orgânica e um sal inorgânico numa razão estequiométrica definida. Os CCIs têm o potencial de alterar propriedades físico-químicas (tais como solubilidade e estabilidade térmica) de um material orgânico puro. Dados recentes mostraram ainda a possibilidade de serem utilizados em resolução quiral.

O objetivo do trabalho apresentado foi o de sintetizar e caracterizar novos CCIs de DL-prolina com halogenetos de lítio, usando técnicas de mecanoquímica e de solução, com o intuito de investigar a capacidade de resolução quiral do lítio. Foi tentada a síntese de diversos co-cristais moleculares e iónicos tanto da L- como da DL- prolina com diferentes sais inorgânicos e moléculas orgânicas, para a obtenção de novos compostos com propriedades modificadas. A difração de raios-X de pó e cristal único, TGA e DSC foram as principais técnicas utilizadas na caracterização dos novos compostos.

Os resultados obtidos confirmam o potencial de resolução quiral do Li através da formação de CCIs, à medida que foram obtidos conglomerados e racematos. Nos CCIs de racematos, pelo menos na estequiometria 1: 1 (prolina: haleto de lítio), observou-se um padrão muito consistente - a preferência homoquiral do lítio resultou na formação de colunas homoquirais nos diferentes CCIs. Já anteriormente descrito na literatura, o CCI da $(DL\text{-}Prolina)_2 \bullet ZnCl_2$ mostrava colunas homoquirais, o nosso interesse aumentou, quando utilizando o nosso procedimento experimental obtivemos um polimorfo, mas sem as colunas homoquirais. Estes resultados estimularam o interesse pelo estudo dos fatores que promovem a formação de colunas homoquirais no empacotamento cristalino - um possível precursor da formação de conglomerados. O estudo e controle dos diferentes factores de cristalização, permitirão no futuro, afinar a co-cristalização de compostos quirais em conglomerados ou em racematos e pavimentar o caminho para novos métodos de resolução quiral, recorrendo a CCIs.

Palavras chave: co-cristal iónico, resolução quiral, prolina, conglomerado

TABLE INDEX

FIGURE INDEX

LIST OF ABBREVIATIONS AND ACRONYMS

API(s) – active pharmaceutical ingredient(s)

CSD – Cambridge Structural Database

CQE, IST – Centro de Química Estrutural, Instituto Superior Técnico

DSC – Differential scanning calorimetry

EM – Erasmus Mundus

EMMC-ChIR or **ChIR** – Erasmus Mundus Master Course in Chemical Innovation and Regulation

PXRD or **XRPD** – Powder X-ray Diffraction

VT-PXRD-Variable Temperature Powder X-ray Diffraction

TGA – Thermal gravimetric analysis

L-Pro-L-Proline

DL-Pro-DL-Proline

SE-Solvent Evaporation

MP-Melting Point

LT-Low Temperature

RT-Room Temperature

LAG-Liquid Assisted Grinding

UniBo – University of Bologna

1 Introduction

1.1 Crystal Engineering

The first use of the term "Crystal Engineering" is attributed to R. Pepepinsky in 1955 and subsequently G. Schmid in 1971, but it was Desiraju who defined it as "*the understanding of intermolecular interactions in the context of crystal packing and the utilization of such understanding in design of new solids with desired physical and chemical properties*".[1] The rapid advance of crystal engineering as a discipline starting in the 1990s was facilitated by technological progress - small molecule crystallography became more accessible, improved computers and point-detectors allowed for a faster and easier manipulation of molecular images, and finally, a more user friendly Cambridge Structural Database (CSD) became the platform for extensive data mining and recognition of repeating interaction motifs in co-crystals. [2] These motifs, later termed "supramolecular synthons" by Desiraju, are "*structural units within the supramolecules which can be formed by known and conceivable synthon operations involving intermolecular interactions*".[1] Based on the components inside them, synthons fall in two main categories: homosynthons in which the interaction is among the same functional groups and heterosynthons-where the two functional groups are different. [1] There is a hierarchy in the evaluation of synthons with the most robust ones being the ones formed from strong and directional interactions, hydrogen and halogen bonds, and only after these synthons have been formed, new weaker and less directional synthons can form.[1] Refer to **Figure *1.1***.

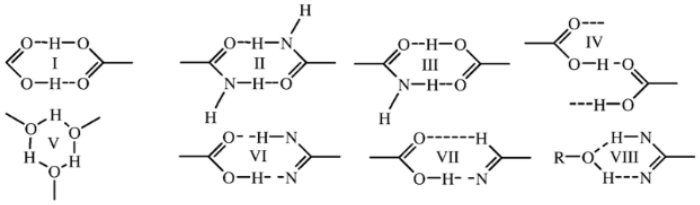

Figure 1.1 Example of the most common homo- and hetero synthons: I is carboxylic acid homosynthon; II an amide dimer homosynthon; III is an acid-amide dimer heterosynthon; IV is a head-to-tale chain formed from carboxylic acids; V is a six-membered intramolecular hydrogen; VI N-H…O and O-H…N synthon; VII C-H…O synthon; VIII is a synthon often observed in diols. [3]

Etter et al.'s extensive study on H-bonds was also a great force towards the advance of crystal engineering as it established the H-bond as both strong and directional. Etters's general rules on hydrogen bonds state that:

1. All good proton donors and acceptors will be used in H-bonding.
2. Six-membered ring intermolecular H-bonds form in preference to intermolecular H-bonds.
3. The best proton donor and acceptors remaining after intermolecular H-bond formation will form intermolecular H-bonds to one-another but not all acceptors will necessarily interact with donors. [4]

1.1.1 Solid State Crystal Forms

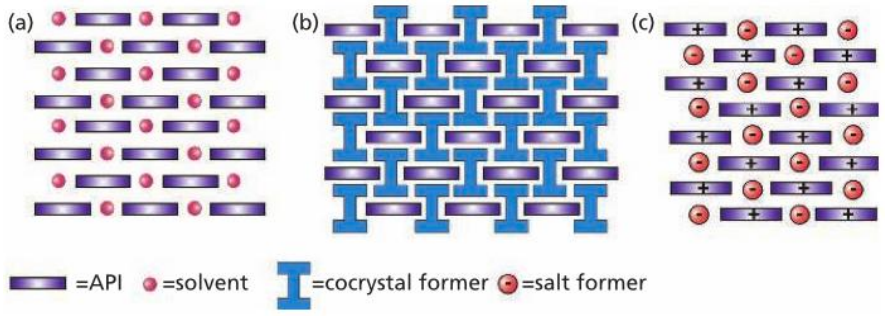

Figure 1.2 Solid State Crystal forms[5]

In fact, it is Etter who is credited for obtaining the first molecular co-crystal by design, using the empirical H-bond rules discussed in the previous section.[6] Before starting our main discussion on co-crystals, it is worth reflecting on the multiple crystal forms that exist in the solid state and have relevance in the pharmaceutical industry and to recognize the differences between them. Starting with the Active Pharmaceutical Ingredient (API), in the solid state we can obtain a salt, various solvates/hydrates and co-crystals. Hydrates and solvates have water or solvent molecules inside the crystal and their physicochemical properties are very different from the ones of the anhydrous molecule.[7] There is still a debate ongoing in industry and academia as to what exactly a co-crystal is, a universal definition still lacking, with the broadest definition being *"a crystalline solid containing multiple components*" and a more specific definition as "*solids that are crystalline single phase materials of two or more different molecular/ionic compounds generally in a stoichiometric ratio which are neither solvates not simple salts*". [8, 9]

Most arguments about the definition challenge what is the nature of the component.[8] Finally, the difference between a salt and a co-crystal, both of them multicomponent crystals, is usually resolved by the question of the proton transfer. If the proton transfer has occurred, the compound is classified as a salt, while if the proton transfer has not occurred- the compound is regarded as a co-crystal.[8] Depending on the nature of the components and the intermolecular interactions, co-crystals fall in two categories- molecular and ionic co-crystals. It should further be noted, that any of these crystal forms can have multiple polymorphs.

1.2 Molecular Co-crystals

The interest of molecular co-crystals is especially high in the pharmaceutical industry where co-crystallizing an API with a molecular co-former can result in the synthesis of a pharmaceutical co-crystal. Since the requirements for salt formation are very different from co-crystallization (it is not necessary that the API is ionizable), co-crystallization can often be achieved even if the API is not ionizable. [9] The new co-crystal forms are an often sought alternative for practical and intellectual property considerations. Co-crystallization can be used to modify the physicochemical properties of the API of interest (e.g., melting point, hygroscopicity/hydration stability and solubility).[10] It can also play an important role in the processing of the drug product final formulations as tablets to achieve suitable hardness/softness, elasticity/plasticity, photo stability and half-life. [6] Finally, it is possible to obtain co-crystals with different stoichiometry between the active and the API- which, on one hand, increases the chance of obtaining a crystal form that more closely matches the physicochemical or pharmacological properties desired for product development, and on the other hand the increased number of API forms increases the patent space around it. [10] The interest is also reflected by the issue of the recent Draft Guidance to Pharmaceutical co-crystals by the United States Food and Drug Administration in August 2016. [11]

1.3 Ionic Co-crystals

An ionic co-crystal (ICC) is a multicomponent crystal system between an inorganic salt and an organic molecule in a defined stoichiometric ratio.[12] The inorganic salts are usually alkaline or alkaline earth salts.[13] Since ICCs combine the properties of molecular crystals with those of salts, they show the potential to provide a route to modified physicochemical properties of the organic material of interest such as solubility, thermal stability, and hygroscopicity with respect to the corresponding neutral molecular crystal.[13, 14]

The formation and stability of the ICC is mainly reliant, on top of ion···ion forces, on (i) dipole···ions interactions between the organic molecule and the cations from the inorganic salt, as oxygen or nitrogen atoms present in the organic molecule are involved in dipole···ion interactions *via* their lone pairs, and on (ii) hydrogen bonds involving hydrogen atoms attached to nitrogen and oxygen and the anions from the inorganic salt.[13]

The prospect of improved product performance, new drug product and formulation development and superior material properties through ionic co-crystal formation make ICCs an area of growing interest in the pharmaceutical and chemical industry.

Most recently, the palette of potential benefits through ionic co-crystal formation has expanded with the addition of chiral resolution. A fascinating discovery was made while exploring ionic co-crystal formation between racemic histidine and lithium halides: the lithium cation exhibited a clear-cut homochiral preference - even though in the unit cell both D-Histidine and L-Histidine are present, the lithium cation is able to separate the enantiomers from each other, choosing to be coordinated by only molecules of single handedness and resulting in infinite "enantiopure" L-His•Li / D-His•Li chains in the racemic ICCs with LiCl and LiBr. Furthermore, even more strikingly the reaction between DL-Histidine and LiI produced a conglomerate of D-Histidine•LiI•H_2O and L-Histidine•LiI•H_2O.[15] Contrastingly, racemate ICCs of DL-Histidine were also obtained with $CaCl_2$ (study to be published separately) but the homochiral preference was not observed - each Ca^{2+} interacts with a molecule of D-Histidine and a molecule of L-Histidine, therefore hinting to the fact that the tetrahedral coordination around the lithium cation has a role in the chiral separation of enantiomers. [16]

1.4 Chirality Importance

Living systems are inherently chiral, and how they interact with chiral molecules whose enantiomers may possess different properties has overreaching implications for the use, safety and regulation of the marketed chiral molecules. Nowadays, although certain advances have been made in asymmetric synthesis, a majority of drugs and agrochemical products is still developed as racemates. Since enantiomers possess identical physicochemical properties but differ in their behavior in biological systems, the enantioseparation of racemates is often challenging yet compulsory. For instance, to obtain approval for their drugs the pharmaceutical companies must obey the strict regulations that guide the authorizations of chiral pharmaceutical compounds and take multiple considerations during drug development. Since opposite enantiomers may possess different pharmacokinetic properties - absorption, distribution, biotransformation and excretion to mention a few - there must be suitable methods to separate the enantiomers, identify and characterize the chiral composition in any material used for pharmacologic / toxicologic and clinical studies to establish the safety of the final product. [17] In the agrochemical industry 25% of all agrochemical products commercialized are chiral, but only 7% are marketed as the single isomer. This highlights the fact that a substantial amount of product is wastefully released to the environment without useful benefit but could potentially cause damaging side effects to non-target organisms. For both industries, single stereoisomer products are favored from the regulatory bodies, intellectual properties (prolonged patent protection for products that underwent a racemic switch) and marketing considerations (greener image for companies, more efficient product use, optimized packaging and transport), but the practical and economical challenges in introducing a single enantiomer product remain. [18] Innovative methods for chiral synthesis and resolution would be needed to address these challenges.

1.4.1 Racemic Mixtures in the Solid State and Chiral Resolution

To better understand the implications of the unexpected finding with Histidine ICC, one should briefly revise how racemic mixtures exist in the solid state and what are the most used methods for chiral separation.

In the solid state racemic mixtures can pack: a) as a racemate, i.e. a racemic compound in which there is an even ratio of both enantiomers in a regularly structured array, b) as a conglomerate, which is a physical mixture of pure enantiomeric crystals, or c) as a *pseudo*racemate (also called a solid solution) in which both enantiomers compete for the same position within the crystal. [19] While a racemic mixture can be found to exist in all three forms, only one of these is thermodynamically stable at given conditions.[20] Spontaneous resolution (conglomerate formation) is a rare phenomenon. It is estimated that only 5-10% of all racemates exist as conglomerates, and that understanding the underlying causes of spontaneous resolution and predicting its occurrence remains "one of the great challenges in stereochemistry" in the 21st century.[20, 21] Investigating conglomerate forming systems is notably advantageous, due to the potential for recovery of the whole enantiomeric excess (ee), recovery of the whole amount of each enantiomer, preferential primary nucleation, and de-racemization in the solid state.[22]

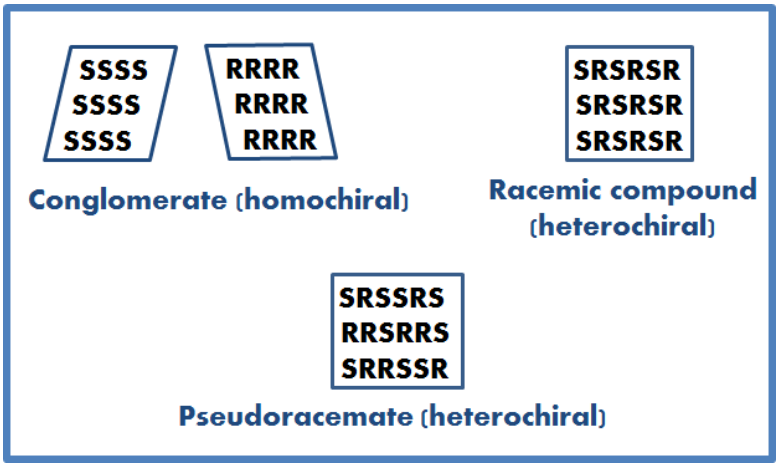

Figure 1.3 Possible solid state phases of racemic mixtures.[19]

From a crystallographic point of view, conglomerates are limited in the number and nature of the space groups they can crystallize in. The presence of conglomerates is compatible only with space groups that lack both reflection and inversion symmetry and thus the number of space groups is decreased to 65 (non-centrosymmetric space groups). The space groups most preferred by enantiomers are monoclinic $P2_1$ and orthorhombic $P2_12_12_1$.[22]

One of the main techniques used for chiral separation is diastereomeric salt formation with a chiral resolving agent, and due to its conceptual similarity with salt formation, co-crystal formation has also been investigated as a novel route towards chiral resolution (refer to **Figure *1.4***). **[23]** The main condition for salt formation in a reaction between an acid and a base is when

ΔpKa = pKa (Acid) - pKa (Base) is greater than 2 or 3, while a co-crystal will generally form if ΔpKa < 0.[8] The strong directionality of the hydrogen bond responsible for co-crystal formation, in combination with the high potential of co-crystallizing compounds that do not easily form salts, promote the chiral separation via co-crystallization as an even more tempting approach.[8] Furthermore, in the particular case of the pharmaceutical industry, co-crystallization of an API with a Generally Regarded as Safe (GRAS) co-former is more advantageous, since there are more GRAS compounds that can be used as co-crystal formers than pharmaceutically acceptable salts. [24] Leyssen et. al have previously demonstrated the enantioselectivity of the co-crystal formation in the case of 2-(2-oxopyrrodin-1-yl)butanamide. S-2-(2-oxopyrrodin-1-yl)butanamide successfully co-crystallized with S-mandelic or S-tartaric acid, but surprisingly did not co-crystallize with neither R-mandelic nor R-tartaric acid. [25] Furthermore, a CSD bibliographic study followed by targeted laboratory co-crystallization experiments estimated that 85% of co-crystal systems behave enantiospecifically.[23] To the best of the author's knowledge, only two studies have previously reported conglomerate formation through molecular co-crystallization. [26, 27] However, none of these studies was performed on ionic co-crystal systems, and conglomerate formation had not previously been reported with a simple Lithium Halide salt as a resolving agent.

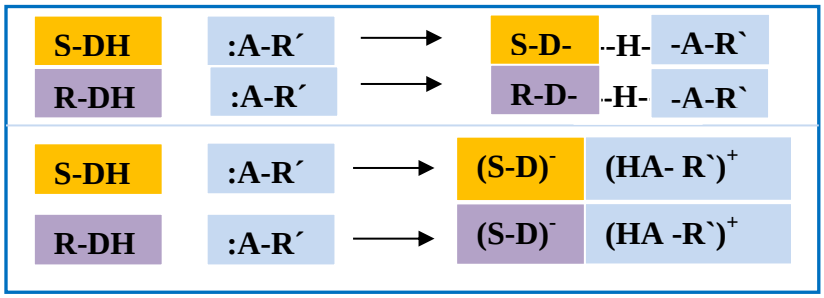

Figure 1.4: Diastereomeric Co-Crystal formation (top) vs. Diastereomeric salt formation (bottom). Diastereomeric co-crystal formation refers to the possibility of co-crystallizing a racemic molecule (S/R) with an enantiopure co-former to obtain co-crystals (no proton transfer) with different physicochemical properties, while with diastereomeric salt formation the idea is to form a salt (proton transfer complete) between the racemate (S/R) and the enantiopure resolving agent to obtain products with different physicochemical properties.

1.5 Synthesis Methods

Several methods have proven useful for the synthesis of co-crystals. In this master thesis, the mechanochemical and solution synthesis have been primarily used.

1.5.1 Mechanochemical synthesis

Mechanochemical synthesis refers to reactions between solids performed via mechanical methods and is suitable for both organic and inorganic compounds. Although it is an ancient method, it has recently been growing in importance both in research and industrial settings as a practical and sustainable method of synthesis.[24] Mechanochemistry can be performed manually, using mortar and pestle, or by a ball mill apparatus. [28] It can be performed in dry (without the addition of solvent) or wet conditions with a catalytic amount of solvent (also known as kneading/liquid assisted grinding or LAG). The addition of a tiny quantity of solvent has been shown to be especially beneficial to enable and increase the rate of product formation.[28] In addition, LAG generally produces materials of higher crystallinity with respect to dry grinding and the choice of solvent can be beneficial to control polymorphism of the starting reagents.[24] The advantages of this technique are that it can be applied on a wide range of chemicals, and it is both economically and environmentally friendly due to the absence or minimal use of solvents; only a small sample quantity is required, and that the final product is obtained in a short time with a high yield.[29] In addition, it has been shown to yield products otherwise not obtainable through solution methods, either due to solubility issues (in cases when the solubility of the reactants is very different with the less soluble reactant crystallizing first) or because of the solvent used disrupting the H-bonds essential for co-crystal formation.[24, 28] The disadvantages are that the reproducibility of experimental conditions such as exact grinding time, temperature and pressure exerted by the operator could be a challenge especially using manual mortar and pestle on a lab scale.[30] The biggest drawback of this technique, however, is the impossibility to obtain single crystals required for structure determination of the novel compound, so that a subsequent crystallization step, helped by seeding, is often required; however, recent advances have made significant improvements to structure solution from powder XRD data. [24, 28]

1.5.2 Solution Synthesis

Co-crystallization in solution is a well-applied method for synthesis. It is generally beneficial in cases when the solubility of the crystal co-formers is similar such as in our work with proline and inorganic salts-both components being very soluble in water. Nevertheless, similar solubility does not necessarily translate to co-crystallization success and besides solubility the polymorphism of the starting reagents should also be considered since using a conformationally flexible co-former can improve the chances of obtaining a novel co-crystal. [3]

1.6 Proline

Proline is a non-essential amino acid abundant in collagen and it is unique among the other amino acids because the amino group is part of a pyrrolidine ring;[31] because of the presence of a secondary amino group it is also called an *imino* acid. The CSD contains the structures for L-Proline, L-Proline monohydrate, DL-Proline and DL-Proline monohydrate. The polymorph of DL-Proline thermodynamically stable at room temperature has also been found by lyophilization.[32] All the structures mentioned above are in their zwitterionic form.

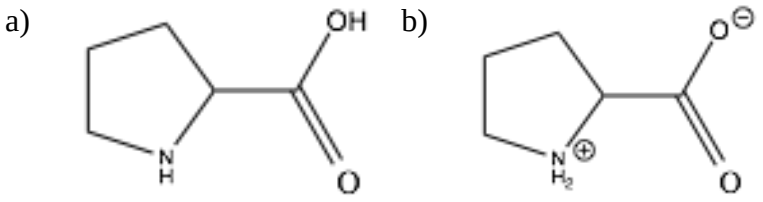

Figure 1.5 Proline in its neutral (a) and zwitterionic (b) forms.

Table 1.1 Unit cell parameters of anhydrous and hydrated forms of enantiopure and racemic proline.

Compound	**L-Proline**	**L-proline Monohydrate**	**DL-Proline**	**DL-Proline**	**DL-Proline Monohydrate**	**DL-Proline Monohydrate**
CSD Refcode	PROLIN	RUWGEV	QANRUT	QANRUT01	DLPROM01	DLPROM02
T (K)	293 K	100 K	120 K	100 K	283-303 K	100 K
Crystal system	Orthorombic	Monoclinic	Monoclinic	Monoclinic	Orthorombic	Orthorombic
Space group	$P2_12_12_1$	C2	$P2_1/c$	$P2_1/c$	Pbca	Pbca
a (Å)	11.550	20.431	8.991	8.795	5.274	5.253
b (Å)	9.020	6.192	5.299	5.293	12.087	11.987
c (Å)	5.200	5.136	11.479	11.340	20.053	19.864
α (º)	90.00	90.00	90.00	90.00	90.00	90.00
β (º)	90.00	95.79	97.04	96.61	90.00	90.00
γ (º)	90.00	90.00	90.00	90.00	90.00	90.00
Volume ($Å^3$)	541.741	646.434	542.699	524.397	1278.315	1250.791

Due to its high solubility, constrained and rigid ring structure and its zwitterionic nature, proline has been investigated as a molecular co-crystal former for pharmaceutical products with fumaric acid, naproxen, celecoxib, C-glycoside derivatives and SGLT inhibitors, among others. [33]

Within the framework of crystal engineering, the pairing of organic and inorganic molecules utilizing ion-ion/ion-dipole and hydrogen bonds to build ICC provides numerous opportunities to enhance the properties of the individual components and is exemplified in the previous studies of proline ionic co-crystal formation. The very first ICC reported between L-Proline and Lithium Salicylate was also evaluated in vivo and showed a better safety profile than the currently marketed Lithium Carbonate API by itself, potentiating the interest of bringing ICCs to the pharmaceutical industry.[34] In addition, ICCs (often referred as "semi-organic" compounds in this branch of chemistry research) have found a place in the growing field of non-linear optics (NLO) as combining organic materials with excellent non-linear optical responses and inorganic molecules with excellent mechanical and chemical properties produces NLO materials with superior properties. [35] As a result hydrated ionic co-crystals between L-proline and LiCl, LiBr, $SrCl_2$, $CaCl_2$ (1:1 stoichiometry amino acid: salt) have been synthesized in solution,

characterized and almost all of them investigated as second order non-linear optical materials. [35-37] Anhydrous ionic co-crystals between L-Proline and LiCl, LiBr (stoichiometry 2:1 amino acid: salt) have been reported as metal-organic materials and $ZnCl_2$, $ZnBr_2$ (stoichiometry 2:1 amino acid: salt) have been investigated for NLO properties. [37-40] Previous studies of ionic co-crystals between racemic proline are limited to two structures - one with $ZnCl_2$ and one with $CaCl_2$ (stoichiometry 1:1 and 2:1 amino acid: $CaCl_2$). To the best of the authors´ knowledge, no ionic co-crystals have been synthesized from enantiopure and racemate proline and LiI. [41] Refer to **Table *1.2*** for crystallographic information on previously reported structures.

Table 1.2 Unit cell parameters for previously reported ICCs of Proline of relevance to this work.

Compound	**L-Pro•LiCl•H_2O**	**L-Pro•LiBr•H_2O**	**L-Pro•LiBr•H_2O**	**L-Pro•$SrCl_2$•H_2O**
CSD Reference	YOXBET	NOCXIO	NOCXIO01	Not in database, R=0.148
Note	193 K	296(2) K	293 (2)K	293 K
Crystal System	Monoclinic, P 2_1	Monoclinic, P 2_1	Monoclinic, P 2_1	Orthorombic, $P2_12_12_1$
a (Å)	7.68 (10)	8.04(7)	8.00(3)	6.70(3)
b (Å)	5.07(5)	5.15(4)	5.14(2)	12.45(5)
c (Å)	10.34(15)	10.62(9)	10.60(4)	15.24(5)
α (º)	90.00	90.00	90.00	90.00
β (º)	105.86(16)	104.25(2)	104.27(2)	90
γ (º)	90.00	90.00	90.00	90
Volume (Å^3)	387.47(9)	425.74(6)	422.12(3)	1271.99
Compound	**(L-Pro)$_2$•$ZnCl_2$**	**(DL-Pro)$_2$•$ZnCl_2$**	**(L-Pro)$_2$•LiCl**	**(L-Pro)$_2$•LiBr**
CSD Reference	DIKVOI	LUPTEV	EVUVUN	EVUVIB
Note	283-303 K	150 (2) K	100 (2) K	100 (2) K
Crystal System Space group	Orthorombic $P2_12_12_1$	Monoclinic, C2/c	Tetragonal, $P4_12_12$	Tetragonal, $P4_12_12$
a (Å)	13.53(3)	18.67(8)	9.08(1)	9.17 (3)
b (Å)	16.26 (3)	5.94 (2)	9.08(1)	9.17(3)
c (Å)	6.60 (1)	13.40 (4)	15.41(2)	15.57 (14)
α (º)	90	104.64(4)	90	90
β (º)	90	90	90	90
γ (º)	90	90	90	90
Volume (Å^3)	1451.491	1438.10 (9)	1270.28(3)	1309.30 (14)

1.7 Objective of the Master Thesis Project

The main objective of this master thesis research project was to synthesize and characterize novel ionic co-crystals of racemic proline with lithium halides using mechanochemistry and solution methods, and to investigate the solid-state chiral resolution power of lithium. This was part of the more general research theme on synthesizing molecular and ionic co-crystals of chiral

and racemic proline with other inorganic salts and organic co-formers to obtain novel compounds with modified properties.

2 Experimental part

All reagents were purchased from Sigma-Aldrich or Alfa Aesar and used without further purification. Milli-Q water was used.

Due to the high hygroscopocity of the salts used, excess amount of salt was used in some of the preparations. Again, due to the high hygroscopicity of the obtained ICCs, some of the powders were dried for several minutes at 70 °C in the oven before PXRD analysis. This is not believed to have influenced the final product.

As some of the compounds already published in the literature were synthesized using solutions methods, the experiments were repeated using mechanochemistry to confirm that the same product could be obtained.

Some of the compounds were synthesized several times to ensure reproducibility and to produce enough material for the experiments. The same compounds were obtained every time, with the exception of a scale up study using LiCl and LiBr, where a mixture of two phases in stoichiometry 1:1 and 2:1 (L-Proline:lithium halide) was obtained. The results from this synthesis are not reported in the tables as the two phases were not separated, and will be discussed in the Unsuccessful Experiments Chapter. Since the solvent used for LAG can determine the product obtained even if it is not present in the final product,[24] some experiments were performed using LAG with methanol, but the same products were obtained as with water, therefore these results will not be reported/discussed.

Finally, it should be noted that the salt LiI is not only hygroscopic, but also very unstable to light, and in open air degrades to lithium and inorganic iodine, also forming multiple hydrated forms. Therefore, using freshly opened anhydrous LiI was found to be crucial to obtain pure ICC phases.

Both L-Proline and DL-Proline are thermally stable until approximately 225°C **Figure *2.1*** below reports the thermogravimetric analysis performed in our laboratory.

a)

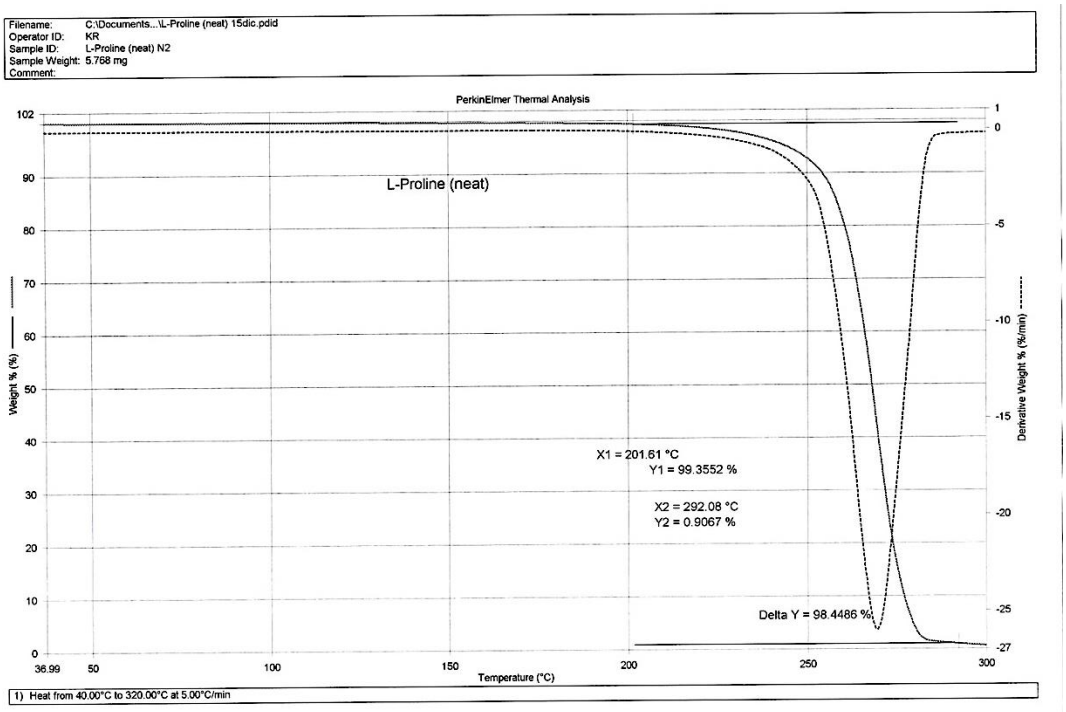

b)

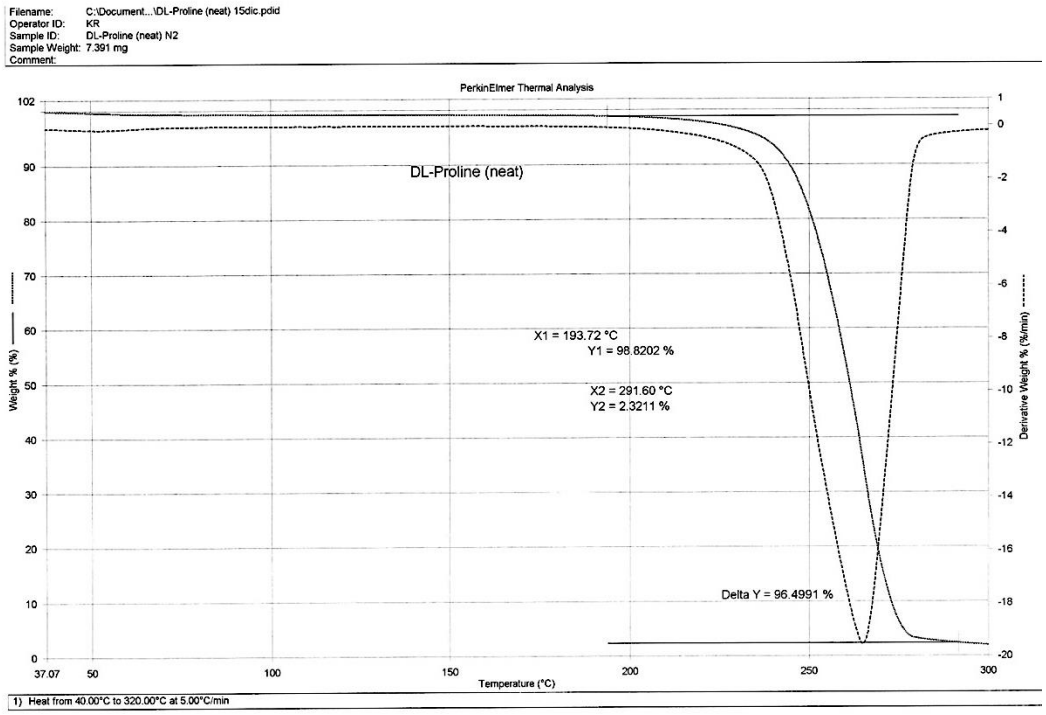

Figure 2.1 Thermogravimetric analysis of a) L-Proline and b) DL-Proline. L-Proline and DL-Proline are thermally stable up to ~ 225°C

2.1 Synthesis using grinding methods

The ICCs were obtained by manually kneading proline (1 mmol) with the inorganic salt (1 mmol) in an agate mortar for 20 min with a drop of water. Since most of the inorganic salts utilized in the project are hygroscopic, limited attempts were made to perform dry grinding, and kneading with a drop of water was preferred. To investigate the kinetic versus the thermodynamic factors in the formation of a racemate ICC versus a conglomerate, for one preparation with LiCl kneading was performed at 5 min intervals, followed by XRD pattern measurement.

The mechanochemically obtained product was then used to grow single crystals for analysis in water or ethanol solution. The preparations in ethanol were stirred and heated to aid the dissolution.

Table 2.1 Summary of successful experiments using mechanochemistry.

Stoichiometry	**Organic Molecule**	**Inorganic Salt**	**Solvent**	**Synthesis Method**
1:1	114.0 mg L-Pro	44.0 mg LiCl	Water	LAG
1:1	58.5 mg L-Pro	46.4 mg LiBr	Water	LAG
1:1	115.1 mg L-Pro	132.2 mg LiI	Water	LAG
1:1	115.3 mg DL-Pro	47.9 mg LiCl	Water	LAG
1:1	115.0 mg DL-Pro	89.5 mg LiBr	Water	LAG
1:1	114.6 mg DL-Pro	133.7 mg LiI	Water	LAG
1:1	118.3 mg L-Pro	48.2 mg LiCl	Methanol	LAG
1:1	116.0 mg L-Pro	93.3 mg LiBr	Methanol	LAG
1:1	115.0 mg L-Pro	142.5 mg LiI	Methanol	LAG
1:1	114.9 mg DL-Pro	49.5 mg LiCl	Methanol	LAG
1:1	116.3 mg DL-Pro	91.7 mg LiBr	Methanol	LAG
1:1	58.1 mg L-Pro	135.0 mg $SrCl_2 \cdot H_2O$	Water	LAG
2:1	231.6 mg DL-Pro	136.4 mg LiI	Water	LAG
2:1	234.6 mg L-Pro	134.6 mg LiI	Water	LAG

2.2 Synthesis using solution methods

Proline (1 mmol) and the inorganic salts were dissolved in several milliliters of water or ethanol and left to evaporate at room temperature as reported in the table below. For both $ZnCl_2$ and $SrCl_2$ the synthesis was first attempted using mechanochemistry, however, a very sticky gel was obtained in the case of $ZnCl_2$ and a film in the case of $SrCl_2$ and it was not possible to further analyze. In water solution, the reaction with $ZnCl_2$ produced a gel, into which crystals suitable for single crystal XRD analysis were identified after more than 6 months. None of the solutions had its pH adjusted.

Table 2.2 Summary of successful experiments using solution methods.

Stoichiometry	**Organic Molecule**	**Inorganic Salt**	**Solvent**	**Synthesis Method**
1:1	118.3 mg L-Pro	46.0 mg LiCl	1 mL Water	SE
1:1	57.1 mg L-Pro	45.4 mg LiBr	1 mL Water	SE
1:1	115.3 mg L-Pro	137.7 mg LiI	1 mL Water	SE
1:1	117.4 mg DL-Pro	46.3 mg LiCl	1 mL Water	SE
	116.1 mg DL-Pro	93.3 mg LiBr	1 mL Water	SE
	1161.1 mg DL-Pro	142.7 mg LiI	1 mL Water	SE
1:1	57.9 mg L-Pro	133.4 mg $SrCl_2 \cdot xH_2O$	3 mLWater	SE
1:1	115.4 mg L-Pro	140.4 mg $ZnCl_2$	Water	SE
1:1	116.5 mg DL-Pro	140.6 mg $ZnCl_2$	Water	SE

2.3 Powder X-Ray Diffraction (PXRD)

X-Ray Diffraction from Powder – University of Bologna. For phase identification purposes, X-Ray diffraction patterns were collected on a PANalytical X´Pert Pro Automated diffractometer equipped with an X´celerator detector in Bragg-Bentano geometry, using Cu-Kα radiation (γ=1.5418 Å) without monochromator in 2θ range between 3º and 50º (step size 0.033º; time/step: 20 s; Soller slit 0,04 rad, antiscatter slit: ½, divergence slit: ¼ ; 40 mA*40kV).

X-Ray diffraction from Powder – Centro de Quimica Estrutual-Lisbon. For phase identification purposes, data were collected using a Brag-Brentano geometry on a Bruker D8Advance powder diffractometer with a copper anode (Cu Kα1, λ=1.5406 Å) and equipped a LYNXEYE-XE detector.

2.4 Variable Temperature Powder X-Ray Diffraction (VT-PXRD)

X-Ray powder diffractograms in the 2θ range between 3º and 50º were collected on a PANalytical X´Pert PRO automated diffractometer equipped with an X´Celerator detector and an Anton Paar TTK 450 system for measures at controlled temperature. The data were collected in open air in Bragg-Brentano geometry using Cu Kα radiation without a monochromator. Thermal programs were selected on the basis of thermogravimetric measurement results.

2.5 Single Crystal X-Ray Diffraction

Single crystals for the hydrated co-crystals and the 2:1 stoichiometry co-crystals were grown by solution evaporation in water or ethanol. Two different Single Crystal Diffractometers were used. Single crystals of the anhydrous co-crystals (1:1 stoichiometry) were grown from powder by dehydrating the powders in a capillary at a temperature below their melting point.

University of Bologna. Single Crystal X-ray diffraction data were collected at room temperature with an Oxford Diffraction X´Calibur equipped with a graphite monochromator and a CCD detector. Mo-Kα radiation (γ=0.71073 Å) was used. Single Crystal data were collected for all compounds. SHELX97 was used for structure solution using direct methods and refinement based on F^2.[42] Non-hydrogen atoms were refined anisotropically. Hydrogen atoms bound to nitrogen and oxygen atoms were either located from a Fourier map or added in calculated positions, and their position was refined riding on their C/N/O atoms. The DL-Pro•LiCl•H_2O and DL-Pro•LiBr•H_2O conglomerate crystals were refined as twinned crystals. The software Mercury 3.8[43] and VESTA 3.3.8[44] have been used to analyze and represent the

crystal packing, and also (Mercury 3.8) to simulate the powder patterns based on single crystal data.

Centro de Quimica Estrutual. Data were collected on a Bruker D8QUEST single crystal diffractometer with Mo sealed tube (Mo Kα, λ=0.71073 Å). The X-ray generator was operated at 50 kV and 30 mA and the X-ray data collection was monitored by the APEX3 program. All data were corrected for Lorentzian, polarization, and absorption effects with SAINT[45] and SADABS[45] programs.

Unit cell parameters for all compounds discussed herein are reported in **Table *2.3***, **Table *2.4***, **Table *2.5***

Table 2.3 Crystallographic data for novel Hydrated Ionic Co-crystals.

	L-Pro•LiCl•H_2O + D-Pro•LiCl•H_2O (conglomerate)	**DL-Pro•LiCl•H_2O (racemate)**	**L-Pro•LiBr•H_2O + D-Pro•LiBr•H_2O (conglomerate)**	**L-Pro•LiI•H_2O**	**DL-Pro•LiI•H_2O (racemate)**	**DL-Pro•$SrCl_2$•$4H_2O$ (racemate)**
Formula	$C_5\ H_{11}\ Cl\ Li\ N\ O_3$	$C_5\ H_{11}\ Cl\ Li\ N\ O_3$	$C_5\ H_{11}\ Br\ Li\ N\ O_3$	$C_5\ H_{11}\ I\ Li\ N\ O_3$	$C_5\ H_{11}\ I\ Li\ N\ O_3$	$C_5\ H_{17}\ N\ O_5\ Sr\ Cl_2$
MW	175.54	175.54	219.99	266.9	266.9	345.72
Crystal System	Monoclinic	Monoclinic	Monoclinic	Monoclinic	Monoclinic	Orthorombic
Space Group	P 2_1	$P2_1/n$	P 2_1	P 2_1	P $2_1/c$	P bca
a (Å)	7.7854(6)	7.7798(7)	8.0080(8)	11.8562(4)	10.9413(10)	14.135(13)
b (Å)	5.1011(3)	5.1002(4)	5.1407(5)	5.2224(2)	5.1757(5)	7.111(11)
c (Å)	10.373(1)	20.1000(14)	10.6122(10)	15.4190(5)	16.988(2)	26.401(2)
α (°)	90	90	90	90	90	90
β (°)	105.436(9)	96.335	104.321(10)	105.337(4)	102.411(10)	90
γ (°)	90	90	90	90	90	90
V($Å^3$)	397.10(6)	792.67(11)	423.29(7)	920.71(6)	939.53(17)	2654(5)
D_c(mg m^{-3})	1.468	1.471	1.726	1.926	1.888	1.731
2θ range	3.80-29.15	2.718-25.415	3.66-28.86	3.46-29.42	3.42-29.23	3.299-29.223
Ncollected./Nunique	1707/1438	6601/1459	1838/1403	4374/2934	3861-2166	3106/3106
Rint.	0.0154	0.0489	0.0295	0.0263	0.0485	0.0322
T (K)	293 (2) K	293(2) K	293 (2) K	293 (2) K	293 (2) K	293 (2) K
R_1 (I>2sigma(I))	0.0837	0.0849	0.0624	0.0342	0.0537	0.0449
wR_2	0.2163	0.2193	0.1396	0.0703	0.0989	0.0712
GOF	1.158	1.080	1.011	0.984	1.002	1.100

Table 2.4 Crystallographic data for the Anhydrous Ionic Co-Crystals (1:1 stoichiometry).

	L-Pro•LiCl	**DL-Pro•LiCl**	**L-Pro•LiBr**	**DL-Pro•LiBr**	**L-Pro•LiI**	**DL-Pro•LiI**
Formula	C5 H9 Cl Li N O2	C5 H9 Cl Li N O2	C5 H9 Br Li N O2	C5 H9 Br Li N O2	C_5 H_9 I Li N O_2	C_5 H_9 I Li N O_2
MW	157.52	157.52	201.97	201.97	248.97	248.97
Crystal System	Orthorhombic	Orthorhombic	Orthorhombic	Orthorhombic	Orthorhombic	Orthorhombic
Space Group	P 2_1 2_1 2_1	P 2_1 2_1 2_1	P 2_1 2_1 2_1	P n a 2_1	P 2_1 2_1 2_1	P n a 2_1
a (Å)	13.0755(3)	13.0596(6)	9.69850(8)	9.70822(15)	5.0904(3)	9.9521(13)
b (Å)	11.3993(3)	11.3501(6)	15.62005(12)	15.6198(2)	9.9978(8)	16.1957(14)
c (Å)	5.03559(12)	5.0431(2)	5.02495(4)	5.02705(8)	16.222(1)	5.0668(5)
α (°)	90	90	90	90	90	90
β (°)	90	90	90	90	90	90
γ (°)	90	90	90	90	90	90
V(Å^3)	750.562(3)	747.53(6)	761.235(11)	762.30(2)	825.58(10)	816.67(15)
D_c(mg m^{-3})	N/A-Structures Solved from Powder data				2.003	2.025
2θ range					28.770	3.24-29.44
Nref./Npara					2138/91	2170/1343
Rint					0.0677	0.0639
T (K)					293 K	293 K
R_1 (I>2sigma(I))					0.1468	0.0723
wR_2					0.1855	0.1359
GOF					1.016	1.026

Table 2.5 Crystallographic data for Anhydrous Ionic Co-Crystals (Different Stoichiometry)

	$(L\text{-}Pro)_2$•LiI	**$(DL\text{-}Pro)_2$•LiI**	**$(DL\text{-}Pro)_2$•$ZnCl_2$**
Formula	$C_{10}\ H_{18}\ Li\ N_2\ O_4\ I$	$C_{10}\ H_{20}\ I\ Li\ N_2\ O_4$	$C_{10}\ H_{18}\ C_{12}\ N_2\ O_4\ Zn$
MW	364.19	370.12	366.55
Crystal System	Orthorhombic	Monoclinic	Monoclinic
Space Group	$P\ 2_1\ 2_1\ 2_1$	P 21/n	P21/c
a (Å)	5.1897(2)	11.499	8.7133(3)
b (Å)	11.5839(5)	5.138	6.6937(3)
c (Å)	24.1467(11)	25.589	25.1323(9)
α (°)	90	90	90
β (°)	90	97.30	94.159(3)
γ (°)	90	90	90
V($Å^3$)	1451.63(11)	1499.6	1461.96(10)
D_c(mg m^{-3})	1.666	1.639	1.665
2θ Range	2.437-28.226	2.809-25.415	3.251-29.532
Nref./Npara	73152/3559	13243/2745	6952/3369
T (K)	273 K	293 (2) K	293 K
Rint	0.0616	0.1065	0.0397
R_1 (I>2sigma(I))	0.0295	0.0963	0.0452
wR_2	0.0665	0.1971	0.0926
GOF	1.102	1.298	1.082

2.6 Thermal Gravimetric Analysis (TGA)

TGA measurements were performed with a PerkinElmer TGA7 in the temperature range 40-500 ºC, under N_2 gas flow and at a heating rate of 5.00 ºC min^{-1}.

2.7 Differential Scanning Calorimetry (DSC)

DSC thermograms were recorded using a Perkin-Elmer Diamond. The samples (1-3 mg range) obtained through kneading were placed in open or closed Al-pans. All measurements were conducted at a heating rate of 10ºC min^{-1}. The initial measurements were performed in an open pan to follow the dehydration processes, and were then repeated in a closed pan to allow the accurate determination of the melting point of the hydrated co-crystals.

Special Thanks to Dr. Katia Rubini for her support with the thermal measurements.

2.8 Structure Determination from PXRD

X-ray diffraction patterns for structure solution for L-Pro•LiCl, L-Pro•LiBr, DL-Pro•LiCl and DL-Pro•LiBr were collected on a PANalytical X'Pert Pro automated diffractometer with transmission geometry equipped with Focusing mirror and Pixcel detector in the 2θ range 3–70° (step size 0.0130°, time/step 170.595 s, Soller slit: 0,04 rad; anti-scatter slit: ½; divergence slit: ½; 40kV x 40mA). The data were analyzed with the software PANalytical X'Pert HighScore Plus and unit cell parameters were found using DICVOL4 or DICVOL algorithms. [46] Simulated and annealing runs with structure fragments were performed with EXPO2014[47]; all options were left as default if not specifically stated and the best solutions were chosen for Rietveld refinements. The structures were refined by the Rietveld method with the software TOPAS5[48], treating the single molecules as rigid bodies and using a spherical harmonics model to describe preferred orientation. Refer to **Table *2.4*** for results.

Many Thanks to Oleksii Shemchuk for helping with solving the structures of all anhydrous compounds.

3 Results and Discussion

The work is organized in several sub-chapters. Each chapter individually describes in detail the structures of the synthesized ICC, reports the results of the performed analysis and is followed by an overall discussion on the chiral resolution obtained through ICC formation and the considerations made during the study to evaluate it.

3.1 Ionic Co-Crystals in 1:1 Stoichiometry Proline: Lithium Salt

3.1.1 DL-Proline•LiCl•H_2O

Kneading DL-Pro with LiCl produced an XRD pattern comparable to the one of the previously reported enantiopure co-crystal with LiCl (CCDC: YOXBET) indicating the formation of a conglomerate. Single crystals suitable for analysis and structure determination were grown through solution evaporation in ethanol. Single crystal results for the analysis of DL-Pro•LiCl•H_2O are reported in **Table *2.3***. The ICC crystallizes in the non-centrosymmetric space group $P2_1$ and has identical unit cell parameters as the previously reported enantiopure ICC, confirming the formation of a conglomerate of L-Pro•LiCl•H_2O and D-Pro•LiCl•H_2O ICCs. Minor differences in volume, angles and lengths could be explained by the experimental setup: conglomerate ICCs were analyzed at room temperature while the enantiopure ICC was analyzed at low temperature. The analysis confirms that a conglomerate was formed, as it shows that the unit cell parameters are identical to the ones previously reported in the literature and because there is only one enantiomer in the unit cell. In the conglomerate crystal, the lithium cation is tetra-coordinated, interacting with three oxygen atoms from three different molecules of proline and one oxygen from a water molecule. Each of the three proline molecules interacts in turn with three lithium cations with the resulting stoichiometry being 1:1. In addition, the relevant hydrogen bonds in this crystalline structure are the amino group forming hydrogen bonds with two chlorine/bromine ions (N-H.....Cl^-/Br^-). Each water molecule forms hydrogen bonds with two anions (O-H.....Cl^-).

Although conglomerate formation was confirmed by single-crystal analysis, the experimental powder pattern of the DL-Pro•LiCl•H_2O was not completely superimposable with the one calculated from the single crystal, which suggested the possibility of a second solid phase. Upon further single crystal screen of crystals grown in water or ethanol, it was confirmed that a racemate ICC was also obtained. The rac-Pro•LiCl•H_2O ICC crystallizes in the centrosymmetric space group $P2_1/n$. The powder pattern calculated from single crystal analysis of the rac-ICC is superimposable to the experimental powder pattern of the kneaded powder. The interactions between the molecules in the unit cell are the same for both ICCs, and although they adopt different space groups, their packings are strikingly similar. The XRD patterns are almost identical for the two ICCs with the exception of several extra "shoulder" peaks in the racemate pattern Refer to **Figure *3.1***.

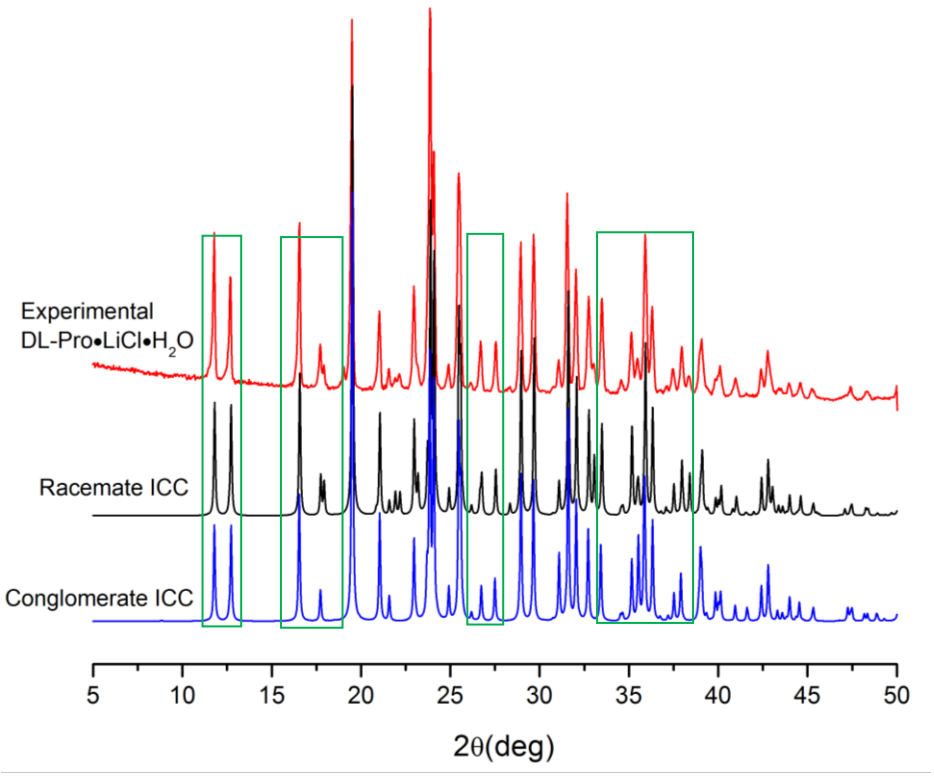

Figure 3.1 Comparison between the experimental powder pattern of DL-Pro•LiCl•H_2O (top), calculated from single crystal, rac-Pro•LiCl•H_2O (middle) and the conglomerate of L-Pro•LiCl•H_2O and D-Pro•LiCl•H_2O (bottom) one calculated by single crystal data (bottom). Differences between the XRD patterns are highlighted in the green boxes.

It is worth noting that while powder X-ray diffraction has a limitation in detecting a mixture of solid phases when the extra phase is below 2% of the total mixture, as illustrated in **Figure *3.1*** there are no extra peaks of conglomerate with respect to the racemate ICC which makes it impossible to determine if the conglomerate and racemate form upon grinding, or the two phases emerge in solution as crystals of conglomerate and racemate ICCs were identified in the same crystallization vial. To investigate the kinetic factor in the solid state, one liquid assisted grinding experiment was performed in which the powders were ground for 5 min and the XRD pattern measured, for a total of 25 min. The results reveal that the racemate ICC forms immediately upon grinding. Refer to **Figure *3.2***.

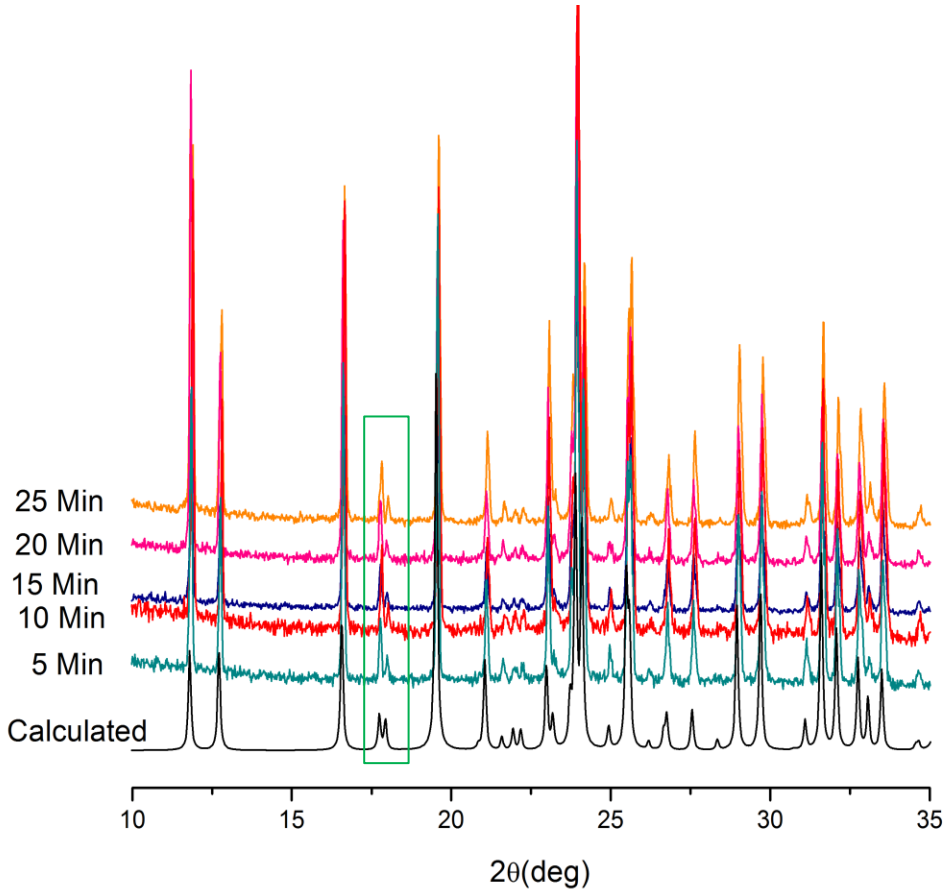

Figure 3.2 Kinetics of DL-Pro•LiCl•H_2O formation. Powder sample was ground with a drop of water for 5 min and XRD pattern. The characteristic racemate doublet peak at 17.6-18.1 2θ range is present already after 5 min of grinding. The calculated XRD pattern corresponds to the racemate DL-Pro•LiCl•H_2O ICC.

The crystallization kinetics of a racemic compound versus a conglomerate in solution should also be considered. As Leyssens et al. discuss, the rate of formation of chiral compounds is reduced as for the growth of a conglomerate crystal the "right" enantiomer must come in contact with a chiral cluster of the same handedness. For any of the two enantiomers it would be easier to come in contact with a racemic cluster in which they will find a matching site.[26] Furthermore, the crystal size is also related to the compound solubility with small crystals (such as the conglomerate ICC) dissolving more readily than large crystals (such as the racemate ICC). [22] If two solid phases are present after grinding, the one that will crystallize first in solution and could potentially serve as a seed for the other crystals is the one with lower solubility (bigger crystal size) which in this case is the racemate ICC. Finally, if we consider crystal growth as an Aufbau

process (one-few-many-nucleus-crystal)[1], and extend it to our conglomerate / racemate system, it is possible to obtain a mid-size enantiopure cluster which is unable to grow further, dissolves and finds an alternative pathway (such as the more efficiently packed racemic crystal).

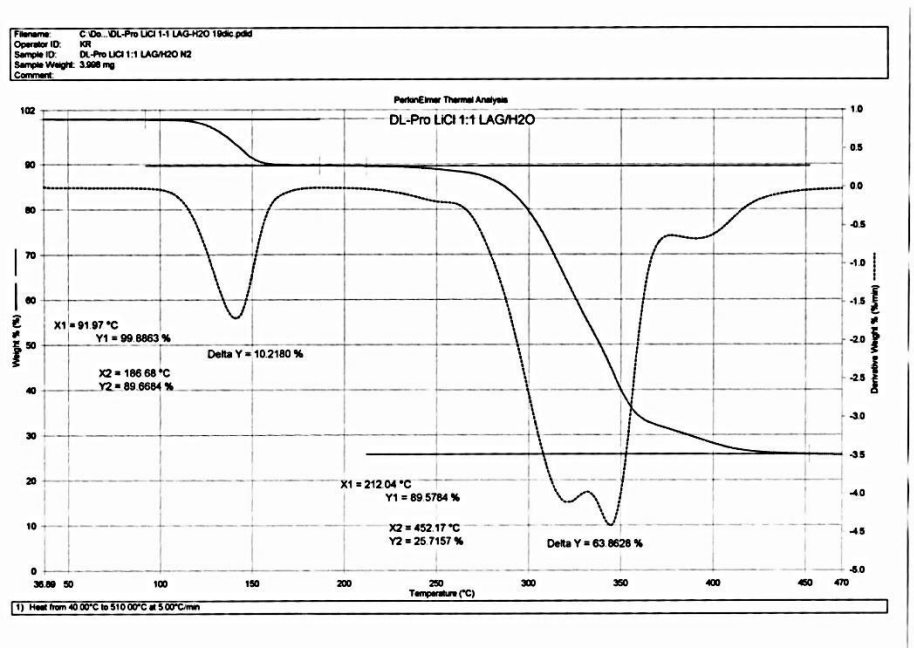

Figure 3.3 TGA trace of DL-Proline•LiCl•H_2O. Analysis shows the loss of 10% sample weight starting at 90°C. As each of the starting reagents has a higher melting point than 90°C and with the knowledge from single-crystal analysis that the ICC is hydrated, this weight loss is assigned to loss of crystallization water.

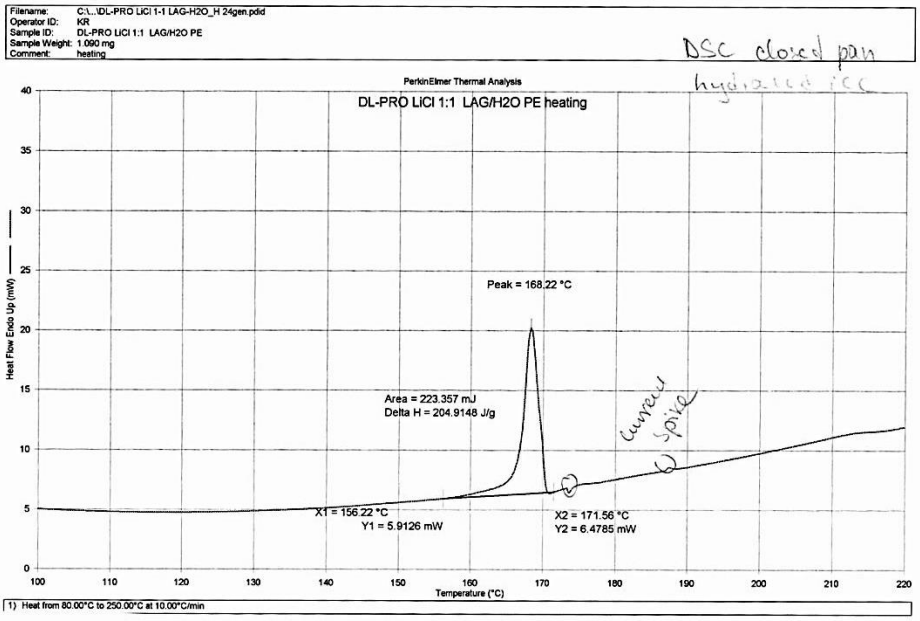

Figure 3.4 DSC (closed pan) Analysis of DL-Proline•LiCl•H_2O.

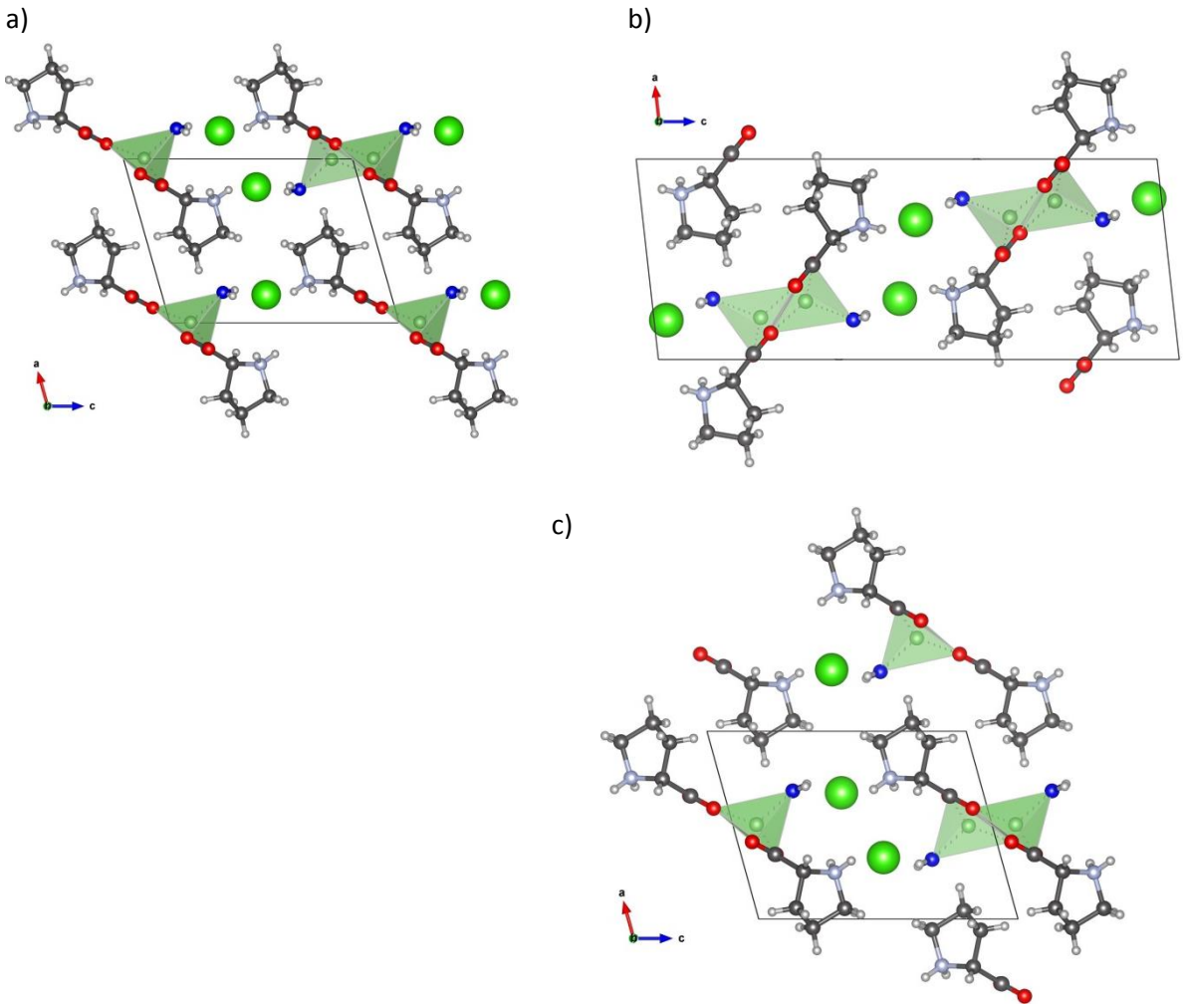

Figure 3.5 a) Packing of L-Pro•LiCl•H_2O (CCDC YOXBET), b) Racemate DL-Pro•LiCl•H_2O and c) Conglomerate of L-Pro•LiCl•H_2O and D-Pro•LiCl•H_2O. The packing arrangement is very similar between the three compounds.

3.1.2 DL-Proline•LiBr•H_2O Conglomerate ICC

Kneading DL-Pro with LiBr produced XRD patterns comparable to those of the previously reported enantiopure co-crystal with LiBr (CCDC: NOCXIO) indicating the formation of a conglomerate. Single crystals suitable for analysis and structure determination were grown through solution evaporation in ethanol. Single crystal results for the analysis of DL-Pro•LiBr•H_2O are reported in **Table *2.3***. The ICC is isomorphous to the conglomerate obtained with LiCl, and crystallizes in non-centrosymmetric space group $P2_1$ and has identical unit cell parameters as the previously reported enantiopure ICC. The analysis confirms that a conglomerate of L-Pro•LiBr•H_2O and D-Pro•LiBr•H_2O was formed, as it shows that the unit cell parameters are identical to the ones previously reported in literature and because there is only one enantiomer in the unit cell. In the conglomerate crystal, the lithium cation assumes a tetrahedral coordination, interacting with three oxygen atoms from three different molecules of proline and one oxygen from a water molecule, each of the three proline molecules interacts in turn with three lithium with the resulting stoichiometry being 1:1. In addition, the relevant hydrogen bonds in this crystalline structure are the amino group hydrogen bonding two chlorine/bromine ions (N-H.....Br^-), which also interact with the two water molecules.

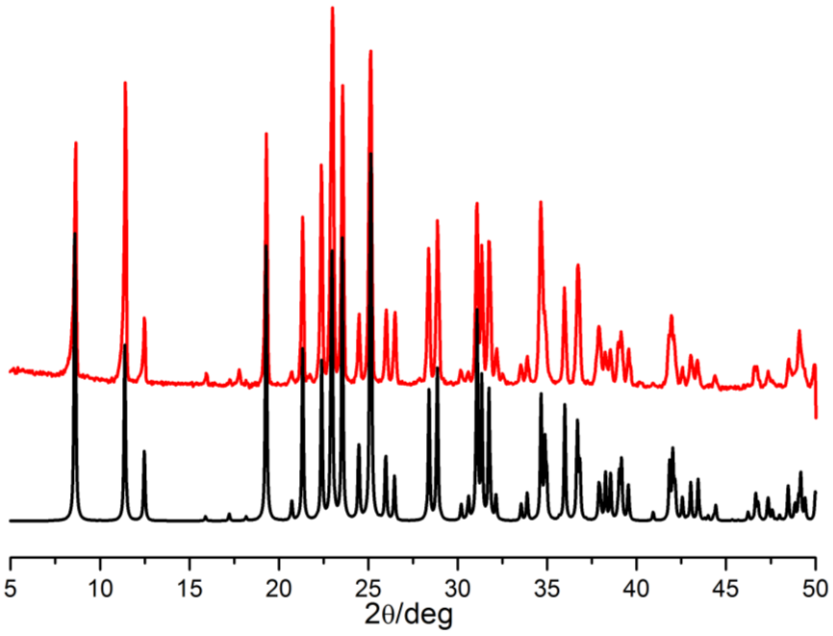

Figure 3.6 Comparison between the experimental powder pattern of conglomerate DL-Proline•LiBr•H_2O (top) and the one calculated by single crystal data (bottom).

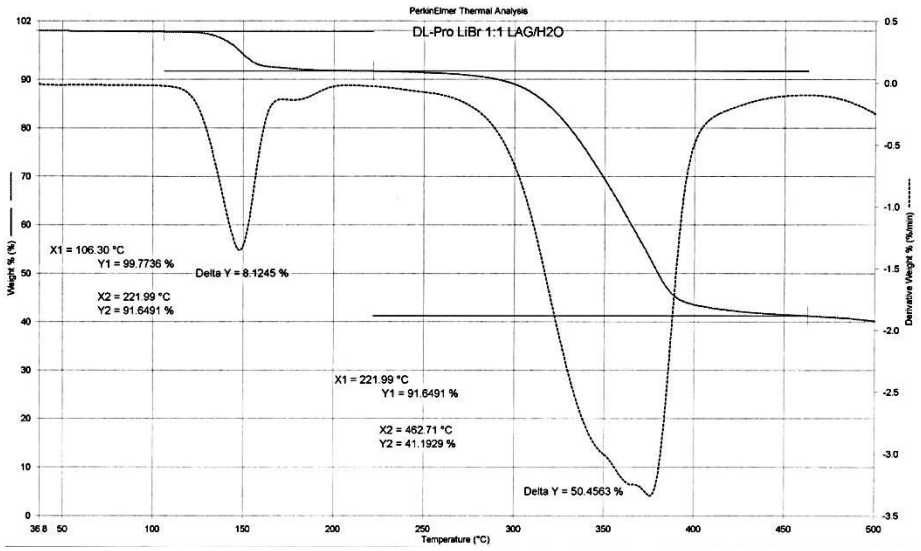

Figure 3.7 TGA trace of DL-Proline•LiBr•H_2O. Analysis shows the loss of 8% sample weight starting at 110°C. As each of the starting reagents has a higher melting point than 100°C and with the knowledge from single-crystal analysis that the ICC is hydrated, this weight loss is assigned to loss of crystallization water.

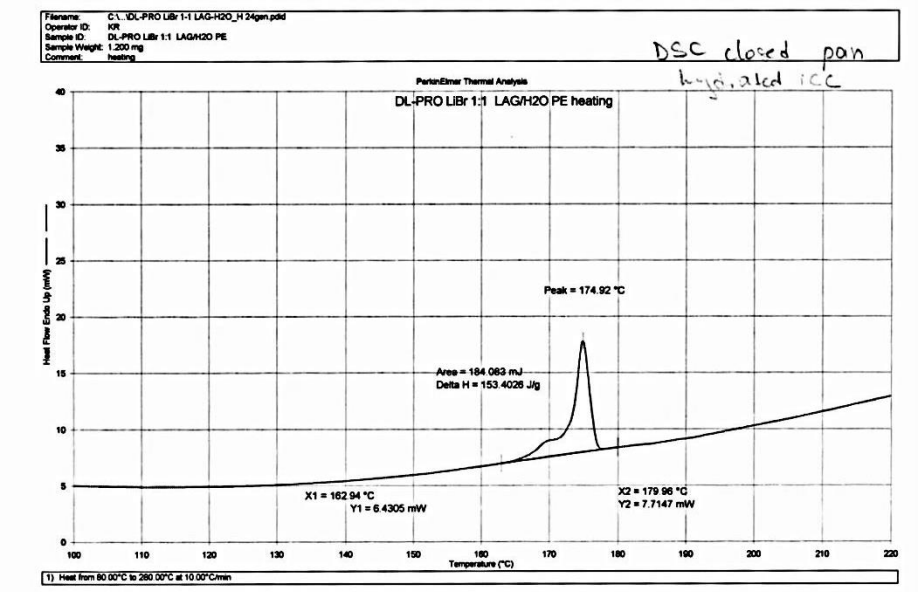

Figure 3.8 DSC (closed pan) Analysis of DL-Proline•LiBr•H_2O.

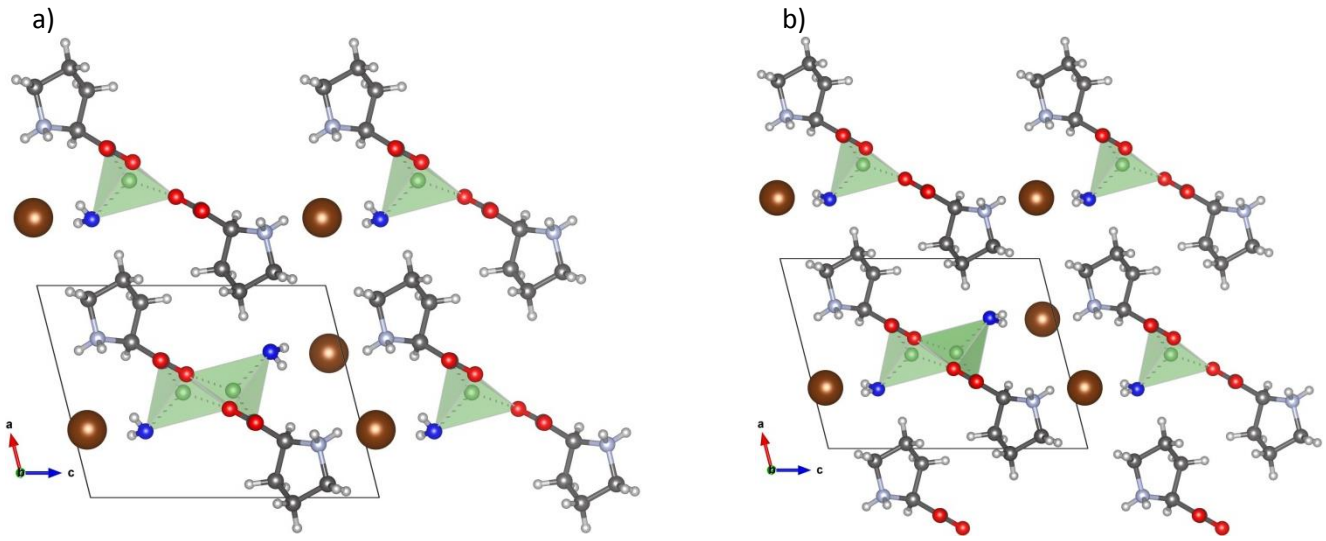

Figure 3.9 Packing of a)L-Pro•LiBr•H_2O(CCDC: NOCXIO, and b)Conglomerate of L-Pro•LiBr•H_2O and D-Pro•LiBr•H_2O.

3.1.3 L-Proline•LiI•H_2O

In the case of LiI, no previous ICC had been reported in the literature with enantiopure L-Proline so we tried to synthesize ICC between both enantiopure and racemic proline and further

investigate whether a conglomerate of ICCs would be formed. L-Pro•LiI•H_2O crystallizes in the non-centrosymmetric space group $P2_12_12_1$ (refer to **Table *2.3*** for details). As in the previously discussed ICCs, the lithium cation assumes a tetrahedral coordination, interacting with three oxygen atoms from three different molecules of proline and one oxygen from a water molecule, each of the three proline molecules interacts in turn with three lithium with the resulting stoichiometry being 1:1. In addition, the relevant hydrogen bonds in this crystalline structure are the amino group forming N-H.....I^- and the water molecules forming O-H.....I^- hydrogen bonds.

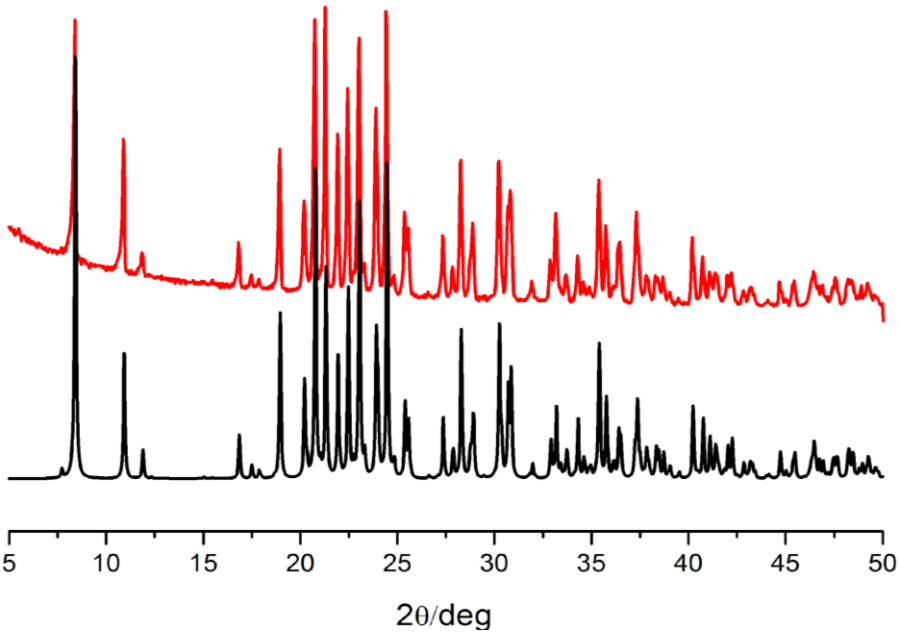

Figure 3.10 Comparison between the experimental powder pattern of L-Proline•LiI•H_2O (top) and the one calculated by single crystal data (bottom).

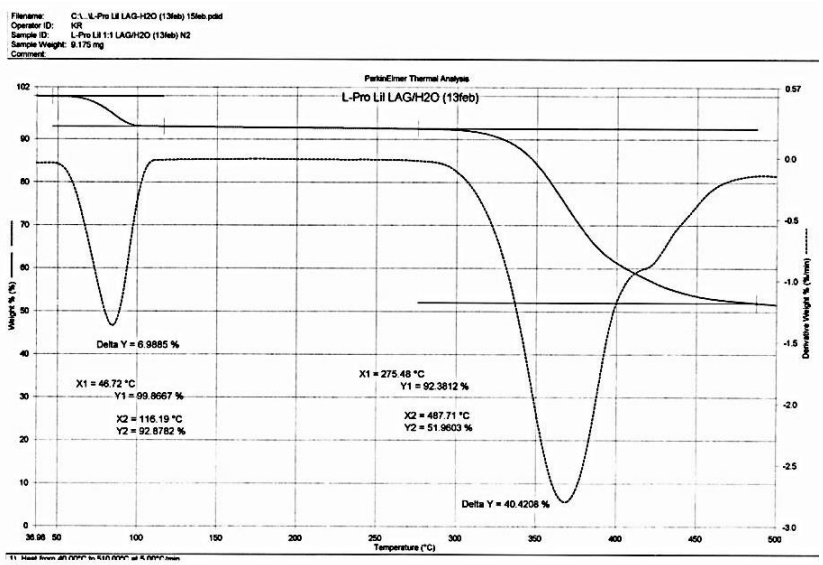

Figure 3.11 TGA trace of L-Proline•LiI•H_2O. Analysis shows the loss of 7% sample weight starting at 50°C. As each of the starting reagents has a higher melting point than 50°C and with the knowledge from single-crystal analysis that the ICC is hydrated, this weight loss is assigned to loss of crystallization water.

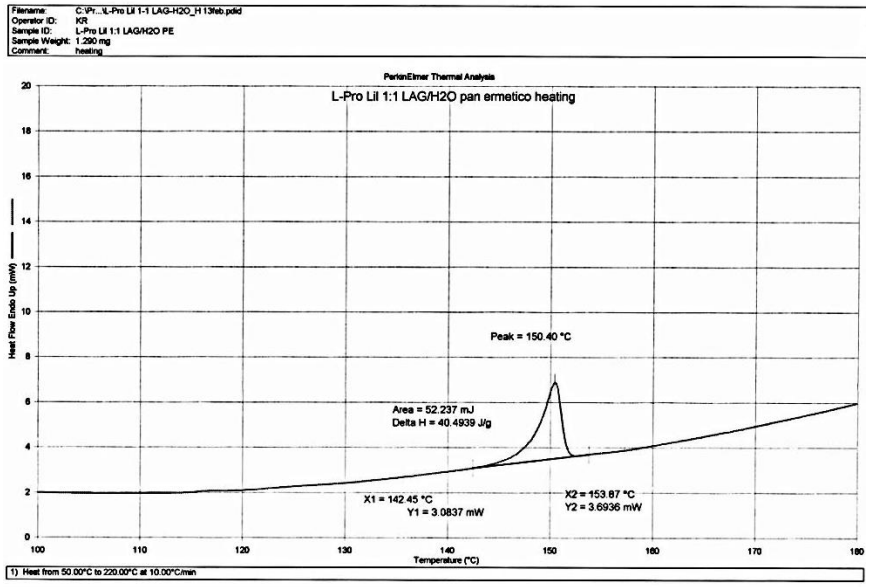

Figure 3.12 DSC (closed pan) Analysis of L-Proline•LiI•H_2O.

3.1.4 DL-Proline•LiI•H_2O-racemic ICC

The powder patterns between the co-crystals with L-Pro•LiI•H_2O and DL-Pro•LiI•H_2O were very different suggesting that, in the case of LiI a conglomerate had not formed and potentially a

racemate ICC had been obtained, which was confirmed by single crystal analysis. The racemate ICC crystallized in an orthorhombic crystal system, in the centrosymmetric space group $Pna2_1$ confirming the presence of both enantiomers in the unit cell (refer to **Table *2.3***).

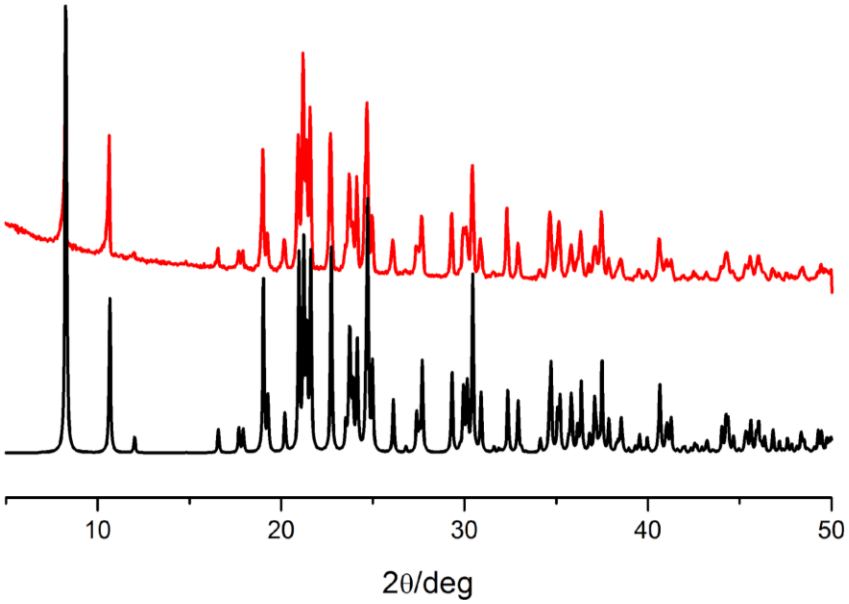

Figure 3.13 Comparison between the experimental powder pattern of DL-Pro•LiI•H_2O (top) and the one calculated by single crystal data (bottom).

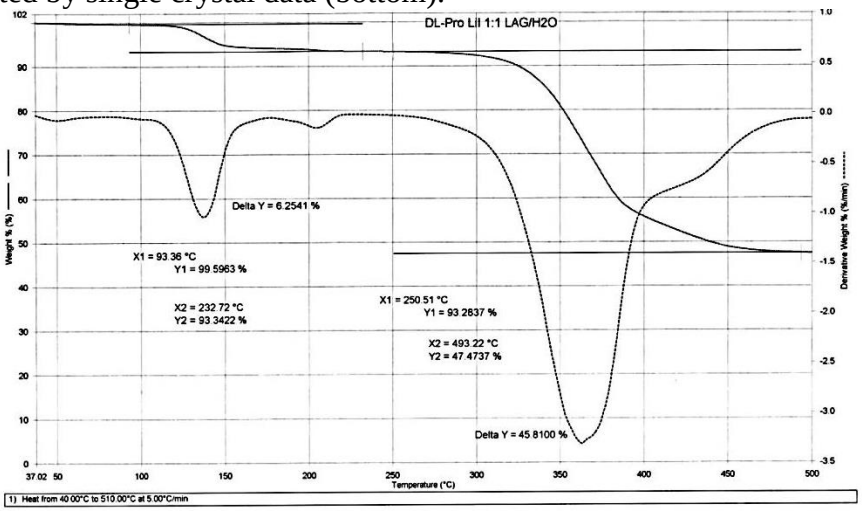

Figure 3.14 TGA trace of DL-Proline•LiI•H_2O. Analysis shows the loss of 6% sample weight starting at 100°C. As each of the starting reagents has a higher melting point than 100°C and with the knowledge from single-crystal analysis that the ICC is hydrated, this weight loss is assigned to loss of crystallization water.

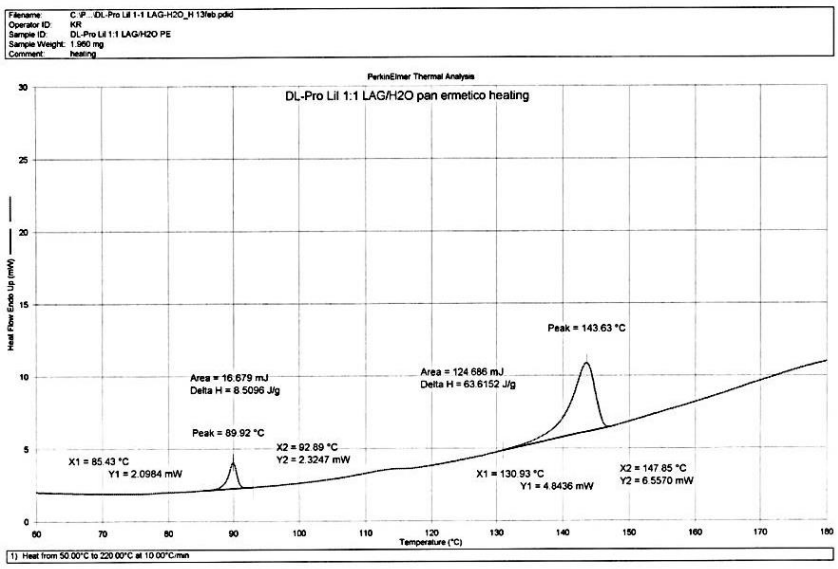

Figure 3.15 DSC (closed pan) Analysis of DL-Proline•LiI•H_2O.

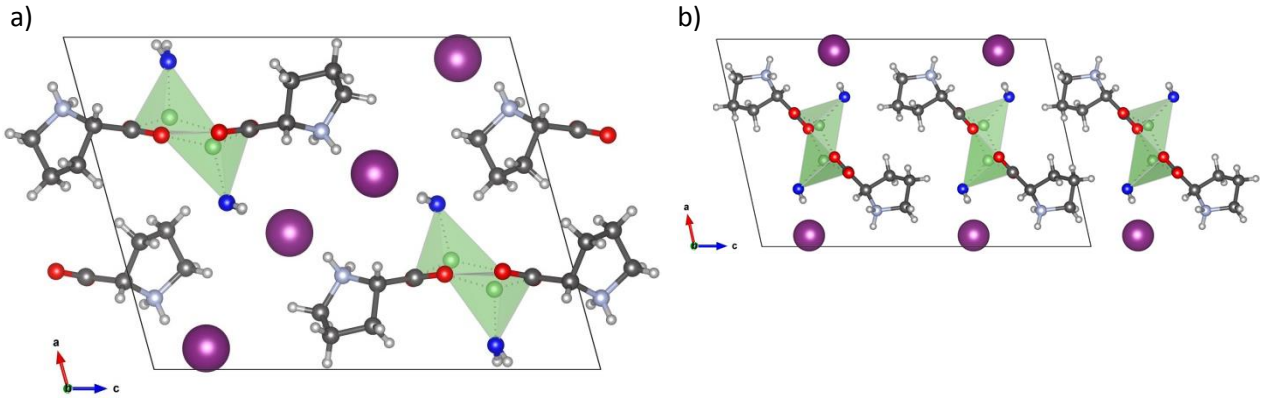

Figure 3.16 a) Packing of L-Pro•LiI•H_2O, and b) Racemate DL-Pro•LiI•H_2O.

3.2 Chiral Resolution in the Solid State

In this research project, the ICC formation between racemic proline and lithium halides has been studied. One of the aims of this work was also that of verifying on a different amino acid the intriguing behavior of L and DL Histidine in the formation of ICCs with LiX (X = Cl, Br, I).

In the true spirit of crystal engineering, a series of ICCs were synthesized and characterized to study the racemate / conglomerate systems and in order to try to understand the role of coordination to the lithium cations and of the other intermolecular interactions in chiral resolution. In the previous work with Histidine, in all structures with lithium halides, Li^+

exhibited a strong homochiral preference by interacting with histidine molecules of single chirality, but only in the case of LiI the homochiral preference resulted in the formation of a conglomerate although the racemic LiCl and LiBr crystals could be described as sort of "co-crystals" of enantiopure chains of L- and D-Histidine with Li^+. This suggested that while the lithium cation coordination played a role in the resolution, the size of the anion and the resulting steric interactions may also be major contribuents ($I^->Br^->Cl^-$). Thus, it was our expectation, that upon repeating the experiment with racemic proline, the same behaviour might be observed. Surprisingly, exactly the opposite happened: a racemic ICC with LiI was formed, a conglomerate with LiBr and both a racemic and conglomerate ICC with LiCl. Nevertheless, even in a small set of compounds such as this one, we were able to identify some consistency in the structural patterns: even though conglomerate and racemate ICCs with lithium halide salts and the amino acids proline and histidine followed different patterns, the homochiral preference of lithium persisted in all structures with 1:1 stoichiometry. In each racemic co-crystal, the lithium cation separates L-Proline/L-Histidine from D-Proline/D-Histidine as each lithium interacts with three amino acid molecules of the same handedness forming infinite enantiopure chains. In the hydrated co-crystals, the enantiopure chains are along the b-axis. One water molecule completes the tetrahedral coordination of the lithium.

Variable Temperature PXRD measurements were also performed on the chiral ICCs and the conglomerate / racemate ICCs to determine their behavior upon dehydration: whether the dehydration process results in decomposition, amorphization, the formation of a stable anhydrous phase and most curiously, whether the conglomerate remains a conglomerate and the racemate ICC remains a racemate. Upon dehydration, all ICCs remain crystalline and the PXRD patterns of the racemate ICCs are comparable to the enantiopure ICCs supporting the hypothesis that the packing remains very similar even when the ICCs have been dehydrated. Nevertheless, the anhydrous phase is not stable and reabsorbs water if left in open air. Refer to **Figure *3.17*** variable temperature XRPD results for all ICCs.

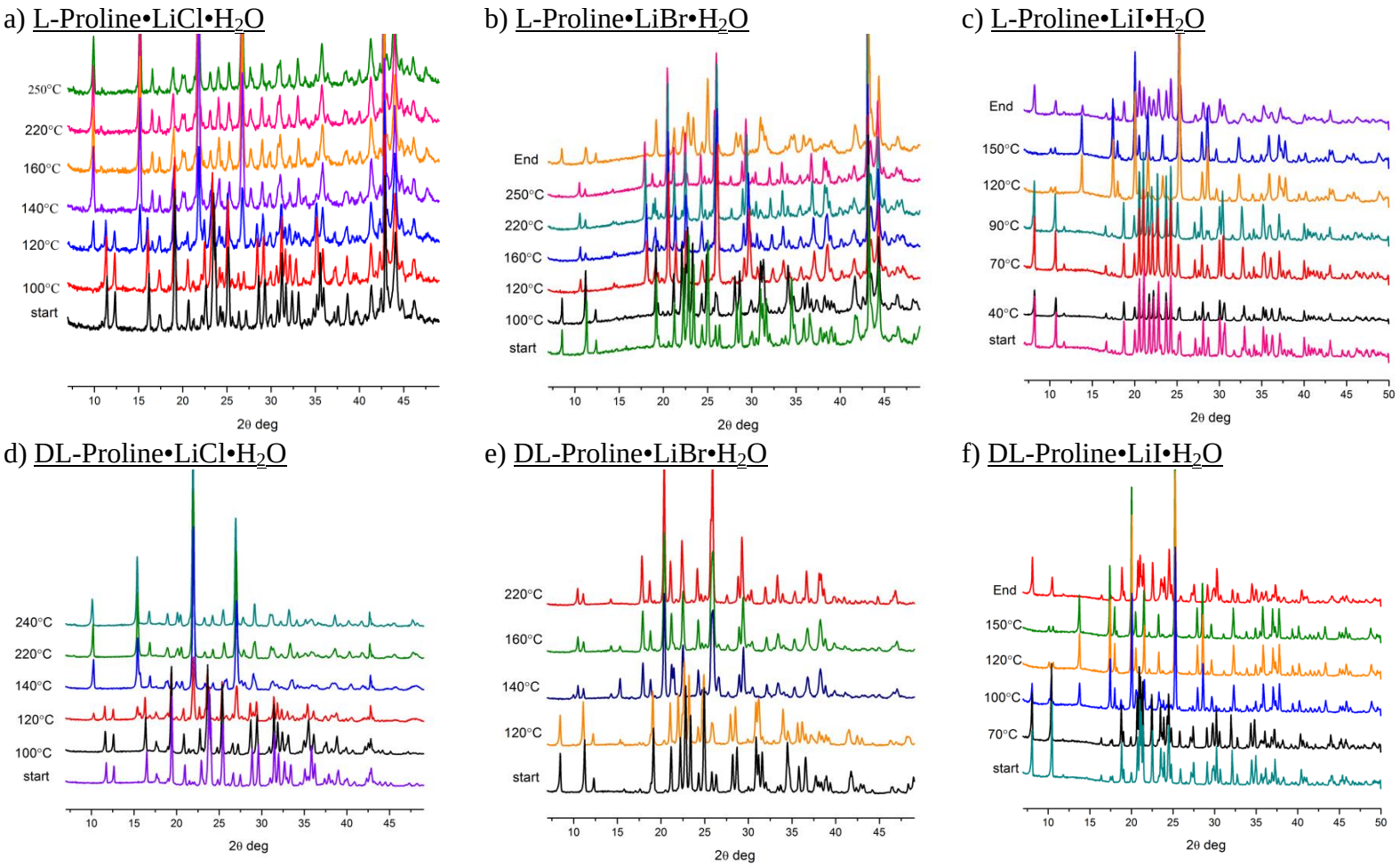

Figure 3.17 Variable Temperature analysis of enantiopure and racemic ICC shows the change in the powder pattern associated with dehydration. All ICCs remain crystalline upon dehydration.

As the variable temperature PXRD analysis revealed that the ICCs remain crystalline even when dehydrated, it was of interest to try and determine the crystal structure of the anhydrous phases and investigate the stability of the enantiopure chains even in the anhydrous structures and to compare the packing patterns to the ones of the enantiopure anhydrous ionic co-crystals. As from the VT-PXRD it was observed that the anhydrous phase, while crystalline, was not stable as it quickly rehydrated back, the idea was to completely dehydrate the powders in a capillary, seal the capillaries and then perform a high-quality capillary PXRD collection for structure solution from powder. This was performed for the enaniopure and racemate ICC with LiCl and LiBr. After dehydration of LiI ICCs at a temperature below their melting point, it was observed that there were crystals formed in the capillary, the capillaries were broken and several crystals with quality suitable for single crystal XRD were found.

To investigate the stability of the pattern, the anhydrous structures of all compounds were determined. Refer to ***Figure 3.18*** for packing representation for all anhydrous structures and to ***Table 2.4*** for unit cell information. As in the hydrated co-crystals the crystal packing in the racemates is strikingly similar to the one of the enantipure ICCs. In fact, the anhydrous phase of the racemate ICC DL-Pro•LiCl•H_2O packs in a non-centrosymmetric space group $P2_12_12_1$ –with unit cell parameters identical to the ones of anhydrous L-Pro•LiCl. Furthermore, the anhydrous phase of the conglomerate of ICCs of L-Pro•LiBr•H_2O and D-Pro•LiBr•H_2O packs in a non-centrosymmetric space group $Pna2_1$ indicating that the compound packs as a racemate in the anhydrous phase. Finally, the individual lithium-proline chains remain enantiopure in the racemate anhydrous structures (with LiBr and LiI). The lithium proline enaniopure chain is preserved along the c-axis in the DL-Pro•LiI•ICC which remained a racemate. As illustrated in **Figure *3.18,*** comparison between the packing patterns of all co-crystals highlights the similarities of the proline – lithium chains in all ICCs and these packing similarities are possibly the driving force for the observed chiral resolution in the solid state and spontaneous resolution.

Conglomerate forming compounds are thermodynamically penalized because there are fewer packing arrangements to accommodate the chiral molecules. Conglomerate formation could thus occur when the packing arrangement between the racemic and the chiral compounds are very similar, such as the case of homochiral columns and comparable packing efficiency.[26] One of Wallach's rules states that a collection of right and left handed objects will be packed more tightly than a collection of homochiral ones. While this rule is disputed due to bias of the

evaluated data set, it has been substantiated at least for resolvable enantiomers and racemic crystals were found to be on average more tightly packed than their chiral counterparts.[49] The packing index of all hydrated and anhydrous structures was calculated to see if it is possible to describe the occurrence and stability of the racemate or conglomerate of ICCs as a result of optimized packing. As illustrated in **Table *3.2*** there are only minor differences in the packing efficiency between the enantiopure, racemate and conglomerate ICCs. In this case, it appears that depending on the conditions each ICC packs in a more stable form.

Thermal analysis was performed on the co-crystals and shows the loss of water from the crystals. DSC analysis was also performed and results provided further insight into the formation of a conglomerate versus a racemate ICC. See ***Table 3.1*** for a summary of melting points of all ICCs. From the thermodynamic point of view, conglomerate formation can be explained by comparing the free energy of formation and the melting point temperature between the enantiopure and the racemic compound.[20] The free energy change for the process of combining two enantiomers to produce a racemic compound has been calculated to be in the range 0 to -2 kcal/mol and is roughly proportional to the difference in the melting points of the enantiopure and the racemic compound. When the melting point of a racemic mixture is more than 20°C lower than the melting point of the enantiopure compound, a conglomerate is formed.[50] DSC analysis was performed on the L-Pro•LiCl•H_2O, and the racemate ICC in a closed pan in order to obtain the melting point of the hydrated compounds. This revealed that there was a 16°C difference between the L-Pro•LiCl•H_2O and the racemate ICC. In addition, this temperature difference below the 20°C threshold for conglomerate formation, can partially explain the formation of both crystal forms and point out to the decisive role of the crystallization conditions (temperature, pressure, solvent, or slight differences in the exact stoichiometry of the reagents) on the resulting mixture of conglomerate and racemate ICCs. [22] For the chiral and conglomerate ICC with LiBr there was a 21°C difference between the L-Pro•LiBr•H_2O and its respective conglomerate which satisfied the thermodynamic requirements for conglomerate formation. Finally, the melting point difference in the case of L-Pro•LiI•H_2O and the racemic ICC DL-Pro•LiI•H_2O was only about 7°C - the smallest difference among the chiral-conglomerate-racemate ICCs studied.

Table 3.1 Summary of DSC results for all ICCs.[1]

	MP (reagent only)	**ICC with LiCl**	**ICC with LiBr**	**ICC with LiI**
L-Proline	233.06°C	183.80°C	195.77°C	150.40°C
DL-Proline	216.08°C	168.22°C	174.92°C	143.63°C
Temperature difference	17°C	16°C	21°C	7°C
Notes	DL-Proline crystallizes as a racemic compound.	Both conglomerate and racemic ICCs have been found.	Only conglomerate has been formed.	Only racemic ICC has been found.

[1] As the enantiopure ICC with LiCl and LiBr have previously been reported and these structures are not discussed in detail in the thesis, the DSC analysis performed on them in our laboratory is reported in the ANNEX.

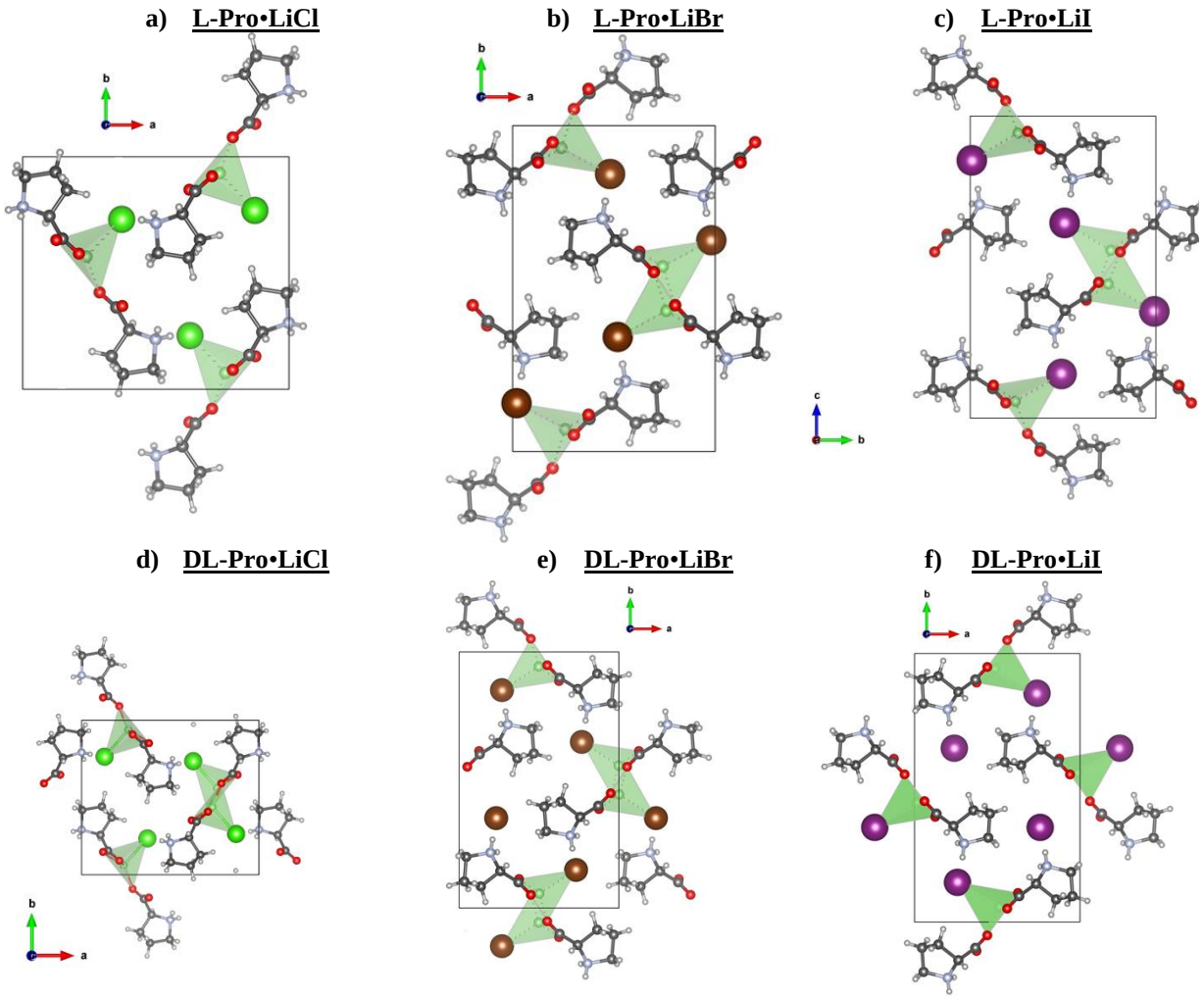

Figure 3.18 Comparison of the Packing arrangement of anhydrous a) L-Pro•LiCl along the c-axis, b) L-Pro•LiBr along the c-axis and c) L-Pro•LiI along a-axis d) DL-Pro•LiCl e) DL-Pro•LiBr f) DL-Pro•LiI.

Table 3.2 Comparison of the packing efficiency (%) of all enantiopure, racemate and conglomerate-forming ICCs.

ICC	Temperature of data collection	Solid State Behavior	Packing Efficiency (%)
L-Pro•LiCl•H_2O (CCDC YOXBET)	LT	Enantiopure	77.0
L-Pro•LiCl•H_2O + D-Pro•LiCl•H_2O	RT	Conglomerate	75.4
DL-Pro•LiCl•H_2O	RT	Racemate	75.0
L-Pro•LiBr•H_2O (CCDC NOCXIO)	RT	Enantiopure	72.5
L-Pro•LiBr•H_2O + D-Pro•LiBr•H_2O	RT	Conglomerate	72.3
L-Pro•LiI•H_2O	RT	Enantiopure	69.7
DL-Pro•LiI•H_2O	RT	Racemate	68.1
Anhydrous Phase of L-Pro•LiCl•H_2O	RT	Enantiopure	71.5
Anhydrous Phase of DL-Pro•LiCl•H_2O	RT	Conglomerate	71.7
Anhydrous Phase of L-Pro•LiBr•H_2O	RT	Enantiopure	72.1
Anhydrous Phase of DL-Pro•LiBr•H_2O	RT	Racemate	71.9
Anhydrous phase of L-Pro•LiI•H_2O	RT	Enantiopure	69.5
Anhydrous phase of DL-Pro•LiI•H_2O	RT	Racemate	70.3

3.3 Ionic Co-Crystal in 2:1 stoichiometry Proline: Salt

3.3.1 Anhydrous ICC (L-Proline)$_2$•LiI

Previously in the literature, anhydrous ionic co-crystals of L-proline and LiCl/LiBr have been reported in the stoichiometry 2:1 amino acid molecules. [38] To be able to compare the packing patterns between all equimolar ICCs and the ones with 2:1, an anhydrous ICC between L-Proline and LiI was obtained through LAG and solved from single-crystal analysis. The ICC crystallizes in space group $P2_12_12_1$. As illustrated in **Figure *3.21***, the packing pattern of the ICC is very different from the one previously reported for the isomorphous structures of L-proline with LiCl and LiBr.

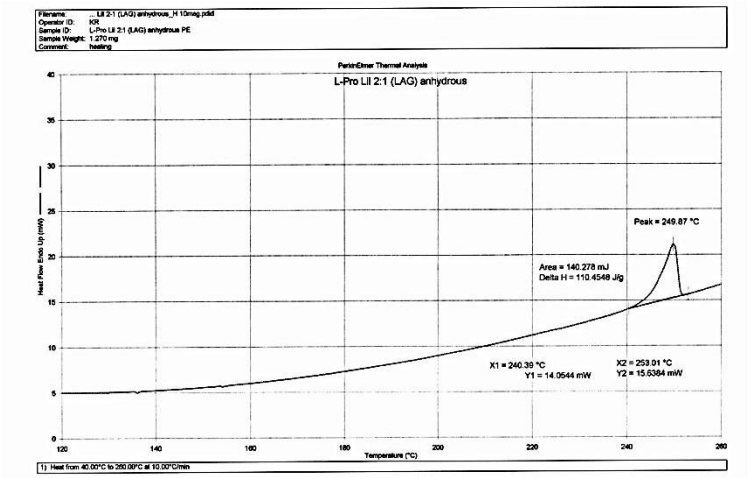

Figure 3.19 DSC (closed pan) Analysis of (L-Proline)$_2$•LiI The ICC has a higher MP than the pure L-Proline reagent.

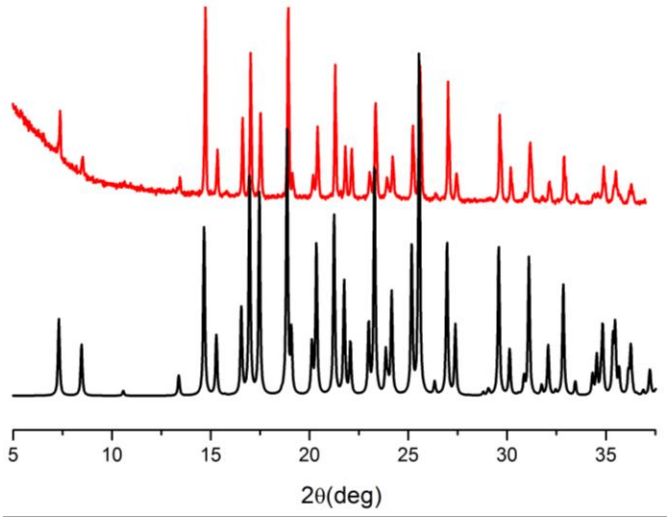

Figure 3.20 The experimental powder pattern of (L-Proline)$_2$•LiI (top) matched the one calculated by single crystal data (bottom).

a) **(L-Pro)$_2$•LiCl** (CCDC: EVUVUN) b) **(L-Pro)$_2$•LiBr** (CCDC: EVUVIB)

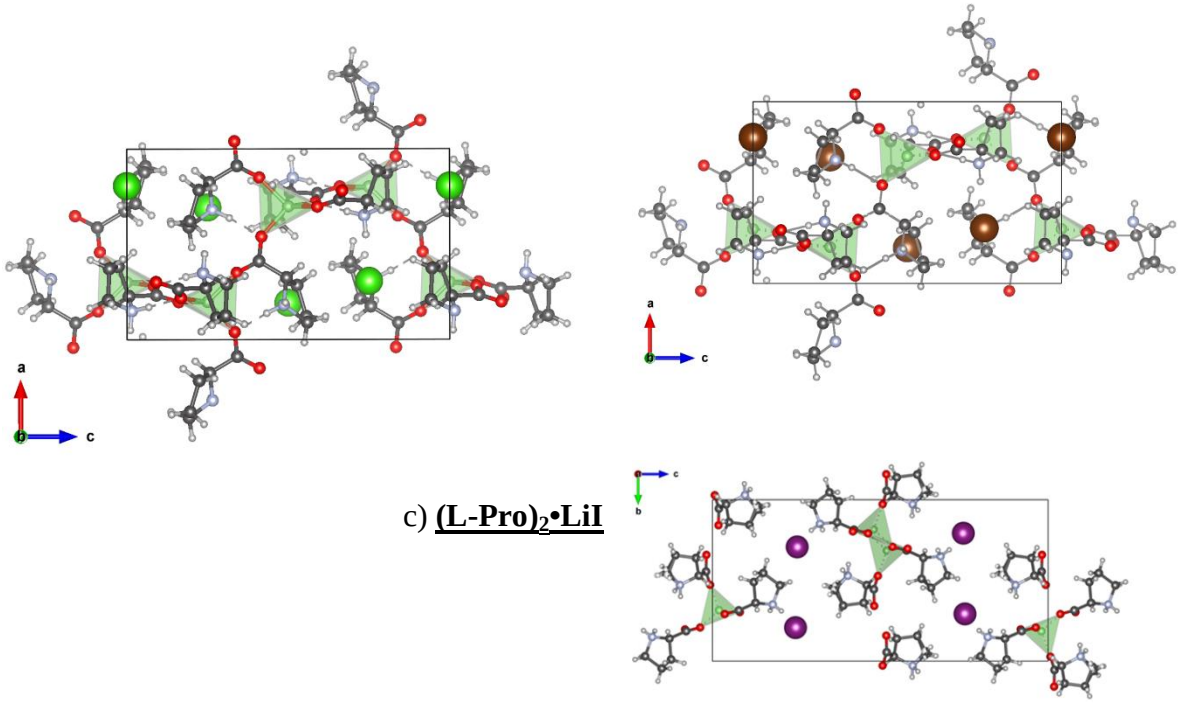

c) **(L-Pro)$_2$•LiI**

Figure 3.21 Comparison of the Packing arrangement of anhydrous a)(L-Pro)$_2$•LiCl (CCDC: EVUVUN), b) (L-Pro)$_2$•LiBr(CCDC: EVUVIB) and c) (L-Pro)$_2$•LiI. The structures with LiCl and LiBr are isomorphous while the structure with LiI follows a completely different packing arrangement.

3.3.2 ICC (DL-Proline)$_2$•LiI

As 2:1 co-crystals between L-Proline and LiCl / LiBr were previously reported and in this work, with LiI synthesized, it was curious to see whether DL-Proline would also co-crystallize in this stoichiometry with the lithium halides and to investigate whether the enantiopure lithium-proline chain would persist or a conglomerate be formed. Surprisingly, co-crystallization with LiCl and LiBr did not result in the formation of a new product. A single crystal XRD unit cell screening of the crystals with LiCl consistently produced only the unit cell of conglomerate ICC, while no crystals of good quality could be obtained from the preparation with LiBr. On the other hand, the reaction with LiI produced a new hydrated racemate ICC co-crystal. Refer to **Table *2.5***. The ICC crystallizes in space group P2$_1$n. In the asymmetric unit, the lithium cation interacts with four proline molecules of both handedness, therefore, in this stoichiometry the enantiopure

chain is not preserved. It should also be noted that the enantiopure ICC L-Pro•LiI in this stoichiometry is anhydrous, compared to the ICC obtained with DL-Proline which has a disordered water molecule. The water molecule does not complete the Li^+ tetrahedral, and it has no coordinating function.

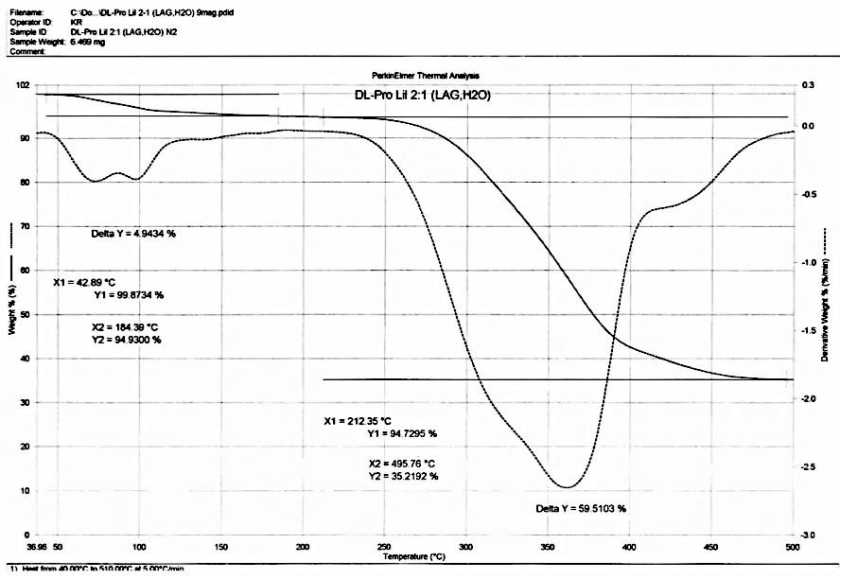

Figure 3.22 TGA Analysis of (DL-Proline)$_2$•LiI. Analysis shows the loss of 5% sample weight starting at 40°C. As each of the starting reagents has a higher melting point than 40°C and with the knowledge from single-crystal analysis that the ICC is hydrated, this weight loss is assigned to loss of crystallization water.

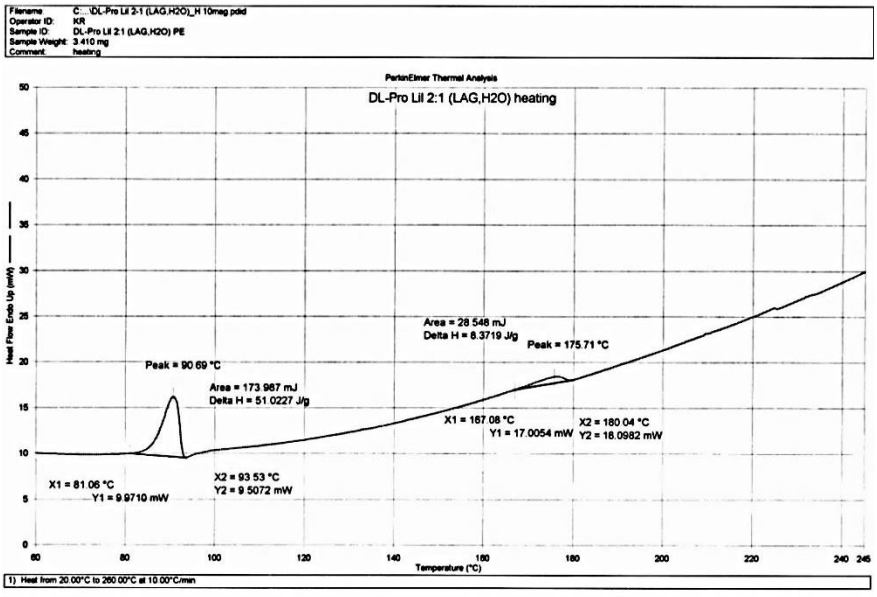

Figure 3.23 DSC (closed pan) Analysis of (DL-Proline)$_2$•LiI. This ICC has a lower MP than the pure DL-Proline.

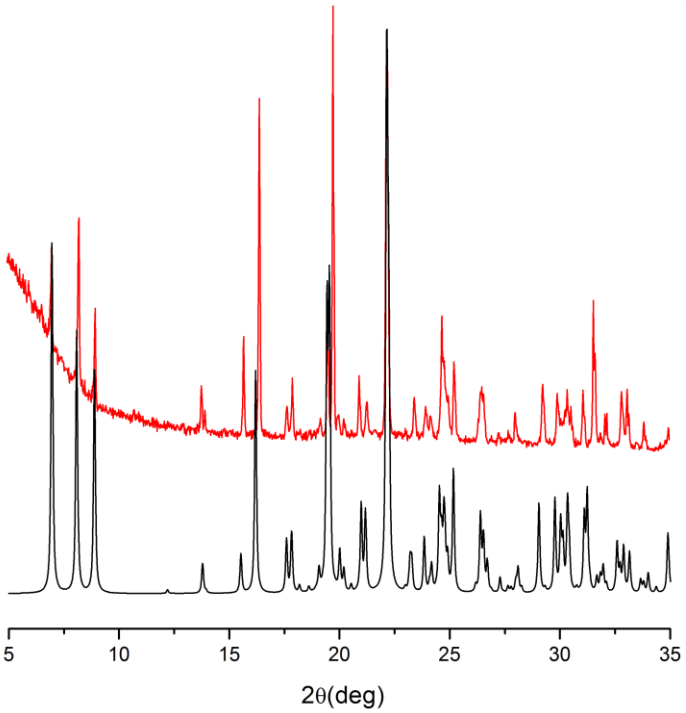

Figure 3.24 The experimental powder pattern of (DL-Proline)$_2$•LiI (top) matched the one calculated by single crystal data (bottom).

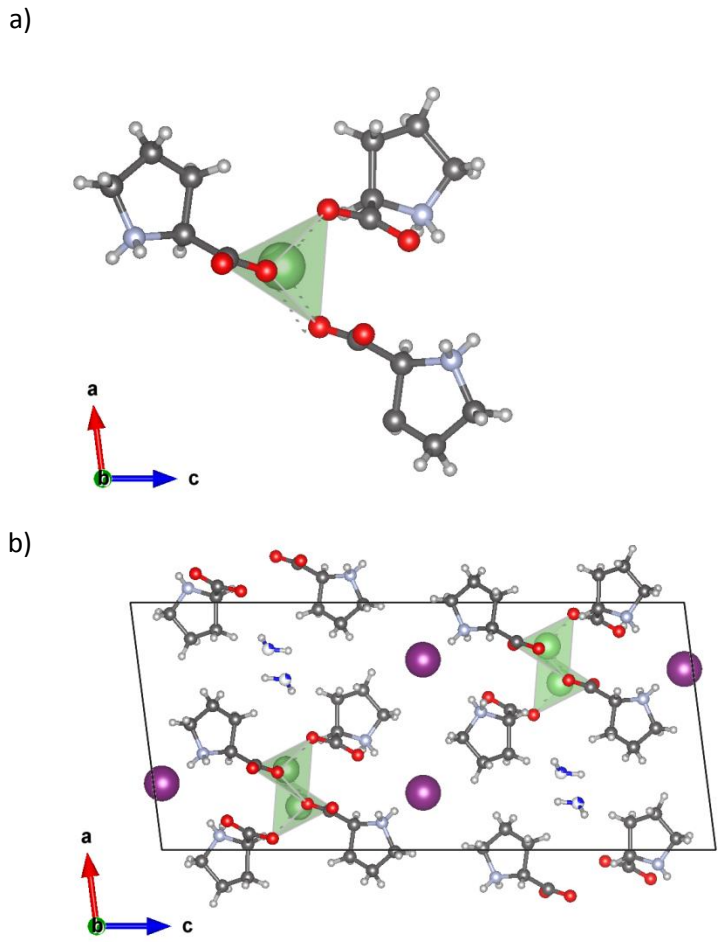

Figure 3.25 a) Tetrahedral coordination around the lithium cation in the $(DL\text{-Proline})_2$•LiI, b) Packing arrangement along the b-axis.

3.4 Other results

3.4.1 Polymorphic ICC $(DL\text{-Proline})_2$•$ZnCl_2$

While the primary objective of our study was to investigate the ionic co-crystal formation between DL-Proline and lithium halides, the general aim was to co-crystallize proline with other inorganic molecules as co-formers. The subsequent literature search produced one structure that specifically caught our attention after our findings with lithium halides and deserved further investigation. There are two structures published for $(L\text{-Proline})_2$•$ZnCl_2$ (CCDC: DIKVOI) and $(DL\text{-Proline})_2$•$ZnCl_2$ (CCDC: LUPTEV) complexes. What is peculiar about this system is that

the authors noted that during a recrystallization experiment with DL-Proline as a starting reagent they observed the XRD patterns of $(L\text{-Proline})_2 \bullet ZnCl_2$ and $(D\text{-Proline})_2 \bullet ZnCl_2$ which, while not explicitly defined by the authors, describes the formation of a conglomerate. The authors then used the conglomerate crystals to seed a preparation between DL-Proline and $ZnCl_2$. The resulting molecule crystallizes in non-centrosymmetric space group C2/c, but in the structure each Zn^{2+} is tetrahedral coordinated with two proline molecules of the same chirality to form infinite homochiral chains - the very same pattern which was observed with lithium halides in our study[40]. Refer to **Table *2.5***. In addition, the packing of the complex is very similar to the ones we have described with the lithium halides - each Zn^{2+} is tetrahedral coordinated with two proline molecules and two chloride anions to complete the tetrahedral, and form a layer in between the Zn-proline chains. As the authors explained the results by the different crystallization conditions and not the identity of the seed crystals, it was imperative to attempt to co-crystallize DL-Proline with $ZnCl_2$ in our laboratory by following a different procedure. As kneading proline with $ZnCl_2$ and a drop of water produced a gel, a solution method was used in which both reactants were dissolved in water at ambient conditions. After 6 months, large rectangular crystals suitable for single crystal analysis were obtained from the gel in the crystallization flask. The new ICC is a polymorph of the original compound and crystallizes in space group $P2_1/c$. Each Zn^{2+} in our polymorph ICC is tetra-coordinated by two proline molecules of different chirality. The relevant hydrogen bonds in this crystalline structure are the amino group donating to one chlorine ion (N-H.....Cl^-) and to oxygen from a neighboring proline molecule (N-H…O).

While in recent years limited number molecular co-crystal polymorphs have been described[51], the number of ionic co-crystal polymorphs is even more limited[52]. To the best of the author's knowledge, this co-crystal is only the second ionic co-crystal polymorph reported. Refer to ***Figure 3.27*** for comparison of Zn^{2+} tetrahedral and packing in the two structures.

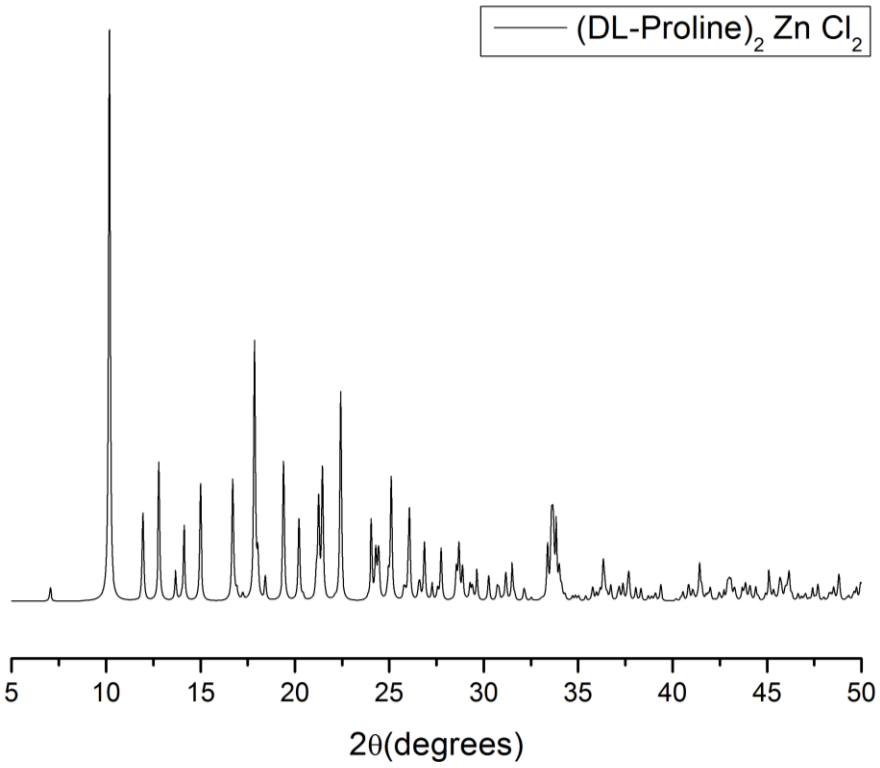

Figure 3.26 Powder Pattern of $(DL\text{-}Proline)_2 \bullet ZnCl_2$ calculated from single crystal XRD.

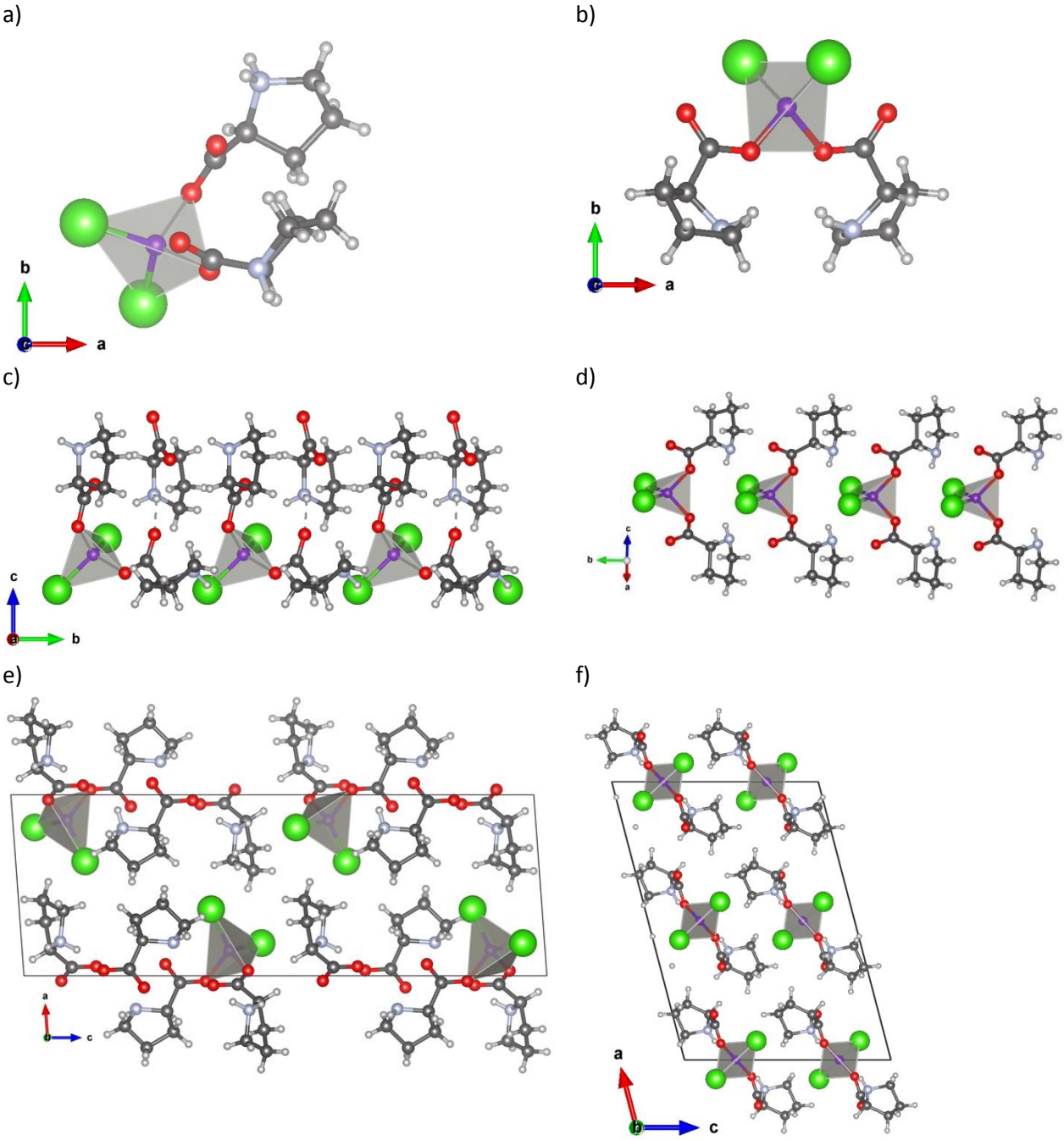

Figure 3.27 a) Zinc cation tetrahedral coordination in the polyrmorph (DL-Proline)$_2$•$ZnCl_2$ ICC. b) Zinc cation tetrahedral coordination in the CCDC LUPTEV (DL-Proline)$_2$•$ZnCl_2$ ICC, c) Chain projection along the a-axis polymorph, d) Chain projection along the a-axis LUPTEV, e) Projection of crystal packing along the b-axis polymorph, f) Projection of crystal packing along the b-axis LUPTEV.

3.4.2 ICC of DL-Proline•$SrCl_2$•$4H_2O$

One strontium cation coordinates one molecule of proline and four water molecules. The relevant hydrogen bonds in this crystalline structure are the amino group donating to two chlorine ions (N-H.....Cl^-). Each water molecule donates to two anions (O-H.....Cl^-).

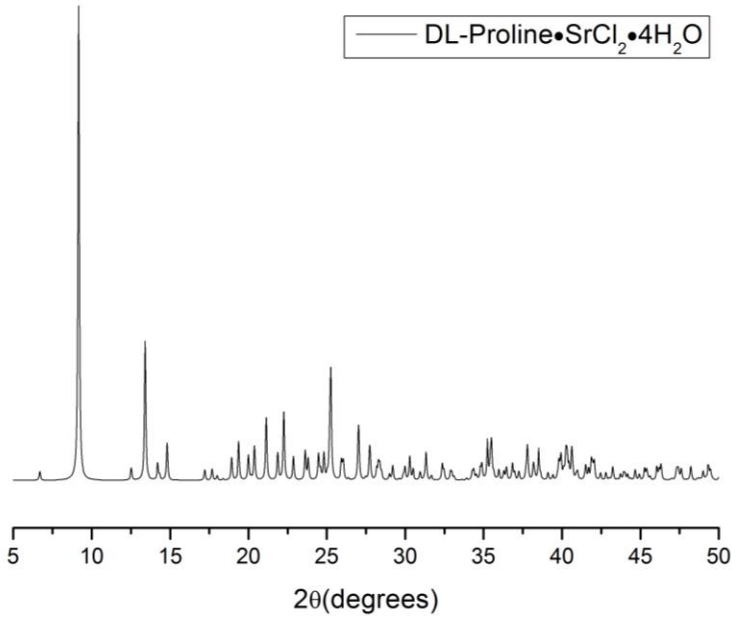

Figure 3.28 Powder Pattern of DL-Proline•$SrCl_2$•$4H_2O$ calculated from single crystal XRD.

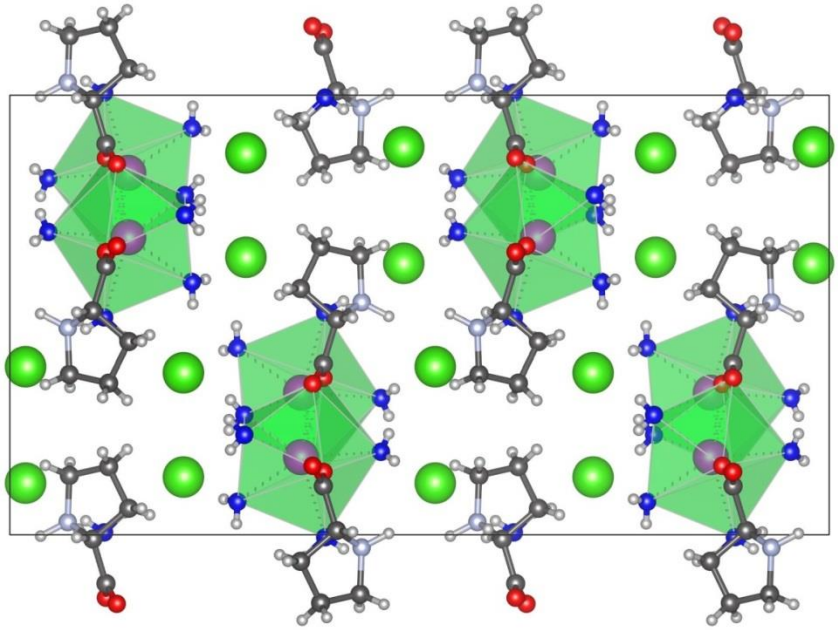

Figure 3.29 Packing DL-Proline•$SrCl_2$•$4H_2O$ along the b-axis.

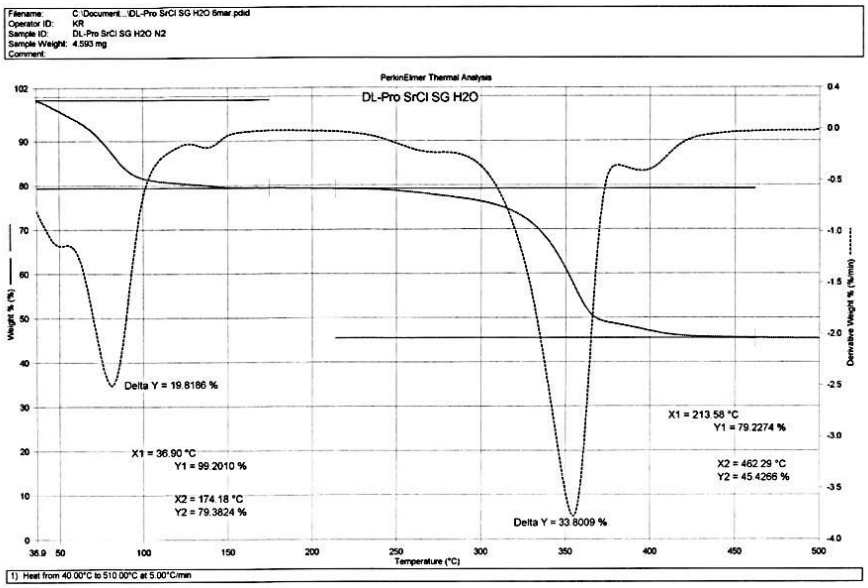

Figure 3.30 TGA trace of DL-Proline•$SrCl_2$•$4H_2O$. Analysis shows the loss of 20% sample weight starting at 40°C. As each of the starting reagents has a higher melting point than 40°C and with the knowledge from single-crystal analysis that the ICC is hydrated, this weight loss is assigned to loss of crystallization water.

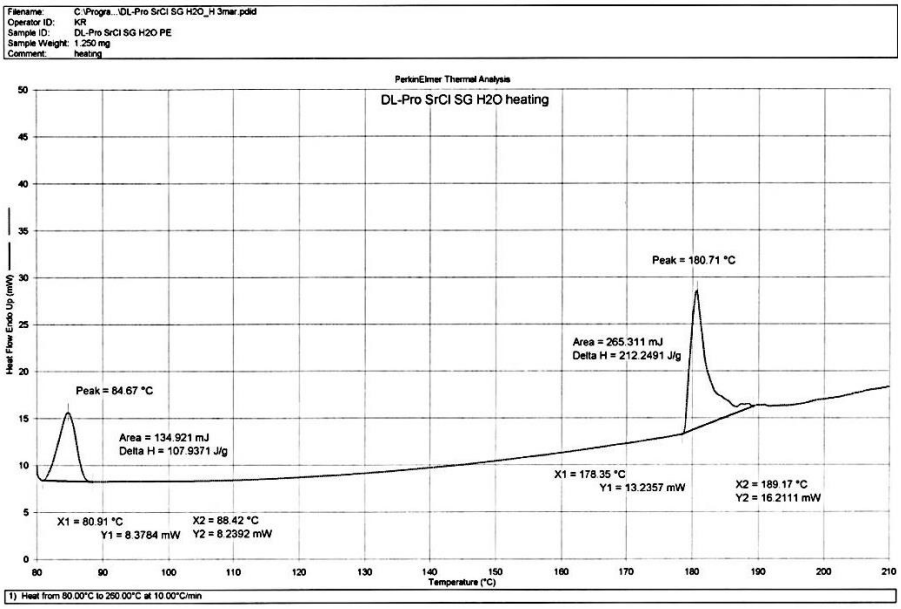

Figure 3.31 DSC (closed pan) Analysis of DL-Proline•$SrCl_2$•$4H_2O$.

3.5 Unsuccessful Experiments

The following sections present the unsuccessful attempts to synthesize ionic and molecular co-crystal during the course of this master thesis.

Following the chiral resolution findings with the lithium halides, it was curious to perform a hetero seeding experiment and determine whether the conglomerate can become a racemate or the racemate become a conglomerate upon seeding with the powder of opposite behavior. However, as proline and the lithium halides are very soluble, the first attempt to perform the seeding was not successful due to lack of sufficient material. It was our idea to scale up the preparations and repeat the seeding but upon scale up, a single phase product was never obtained –a mixture of 2:1 and 1:1 Proline: Lithium Halide ICCs was obtained. Although several attempts were made to recrystallize and separate the phases, this proved not possible within the time limitations.

3.5.1 Ionic Co-crystals

Table 3.3 Synthesis of ICCs: Cases of unsuccessful reactions.

Stoichiometry	**Organic Molecule**	**Inorganic Salt**	**Solvent**	**Synthesis Method**	**Result**
1:1	114.7 mg L-Pro	131.8 mg NaCl	n/a	Dry grinding	Physical mixture
1:1	58.0 mg L-Pro	137.6 mg $CaBr_2$ x H_2O	Water	LAG	Film upon drying
1:1	58.6 mg L-Pro	131.8 mg $SrCl_2$ $6H_2O$	n/a	Dry grinding	Poor crystallinity
1:1	58.0 mg L-Pro	137.6 mg $CaBr_2$ xH_2O	Water	LAG	A film was obtained
1:1	57.3 mg L-pro	133.7 mg $SrCl_2$ $6H_2O$	ACN	LAG	A gum like compound.
1:1	115.6 mg L-Pro	111.3 mg $CaCl_2$	Water	LAG	Product already described in the literature
1:2	115.8 mg L-Pro	84.2 mg LiCl	Water	LAG/SE	Powder too hygroscopic to analyze, single crystals to unstable for collection
1:2	116.3 mg L-Pro	174.1 mg LiBr	Water	LAG/SE	
1:2	58.3 mg L-Pro	156.7 mg LiI	Water	LAG/SE	
1:2	116.2 mg DL-Pro	85.8 mg LiCl	Water	LAG/SE	
1:2	115.3 mg DL-Pro	178.9 mg LiBr	Water	LAG/SE	
1:2	57.3 mg DL-Pro	160.0 mg LiI	Water	LAG/SE	
1:1	113.6 mg L-Pro	144.5 mg $ZnCl_2$	Water	LAG	Very sticky powder

3.5.2 Molecular Co-crystals

Table 3.4 Synthesis of molecular co-crystals: Cases of unsuccessful reactions.

Stoichiometry	**Organic Molecule**	**Organic Molecule**	**Solvent**	**Synthesis Method**	**Result**
1:1	116.4 mg DL-Pro	134.6 mg L-Aspartic Acid	100 μL Water	LAG	Physical mixture
1:1	116.2 mg DL-Pro	116.2 mg L-Glutamic Acid	100 μL Water	LAG	Physical mixture
1:1	115.2 mg DL-Pro	146.0 mg L-Glutamine	100 μL Water	LAG	Physical mixture
1:1	155.5 mg DL-Pro	151.1 mg L(+)Tartaric Acid	100 μL Water	LAG	Sticky gel
1:1	116.4 mg DL-Pro	134.6 mg L-Aspartic Acid	Water	SE	Physical mixture
1:1	116.2 mg DL-Pro	116.2 mg L-Glutamic Acid	Water	SE	Physical mixture
1:1	115.2 mg DL-Pro	146.0 mg L-Glutamine	Water	SE	Physical mixture
1:1	115.3 mg DL-Pro	148.8 mg L(+)Tartaric Acid	Water	SE	gel
1:1	197.1 mg L-DOPA	116.3 mg L-Pro	70 mL Water	SE	No new crystals obtained, only crystals of the starting reagents
1:1	197.6 mg L-DOPA	117.8 mg DL-Pro	70 mL Water	SE	
1:1	90.5 mg L-Ascorbic Acid	58.3 mg DL-Pro	Water	SE	No new crystals obtained, only crystals of the starting reagents.

Conclusions

In this master research thesis, two objectives were followed: to investigate the homochiral preference of the Li^+ and to obtain novel ionic or molecular co-crystals.

For the chiral resolution power of lithium halides several ICCs were synthesized and fully characterized by single-crystal and powder x-ray diffraction, thermal analysis and their packing efficiency was calculated. The results highlight that indeed Li^+, at least when used in 1:1 stoichiometry with rac-Proline, is consistent in its homochiral preference. When co-crystallized with LiCl and LiBr, a conglomerate of ICCs was formed, while with LiI a racemic ICC is formed. In addition, a rac-ICC with LiCl was obtained. In all racemic-hydrated or anhydrous ICC structures, in 1:1 stoichiometry, the lithium-proline chains were enantiopure and had a packing pattern and efficiency very close to the enantiopure ICCs. It is thought that the spontaneous resolution is made possible due to these packing similarities. These results seem to confirm the proposed potential for chiral resolution through ICC formation, and encourage further research to establish the homochiral preference of lithium cation and studying the factors and conditions that promote chiral resolution through ionic co-crystallization. More studies are needed to be able to fine-tune these conditions to use in chiral resolution.

As part of the general theme of the thesis, several novel ICCs were synthesized with enantiopure and rac-Proline with LiI, $SrCl_2$ and $ZnCl_2$. All of the co-crystals exhibited thermal properties different than the pure reagents highlighting once again the potential to modify the physicochemical properties of the organic molecule of interest though ICC formation. The particular case of $(DL\text{-}Pro)_2 \bullet ZnCl_2$ also underlines the possibility of obtaining homochiral or heterochiral chains as a result of different crystallization conditions. This result is bringing us one step closer to chiral resolution, leading us to engineering enaniopure chains in an ICC.

Unfortunately, although several attempts were made to co-crystallize Proline with other amino acids, all of them resulted in a mixture of starting reagents. This highlights the fact that although we can use homo- and hetero -synthons to predict interactions between the molecules, novel products may not always be obtained.

BIBGLIOGRAPHY

[1] G. R. Desiraju, *Journal of the American Chemical Society* **2013**, *135*, 9952-9967.

[2] N. Shan, M. J. Zaworotko, *Drug Discovery Today* **2008**, *13*, 440-446; D. Braga, *Chemical Communications* **2003**, 2751-2754.

[3] N. Blagden, M. de Matas, P. T. Gavan, P. York, *Advanced Drug Delivery Reviews* **2007**, *59*, 617-630.

[4] M. C. Etter, *Accounts of Chemical Research* **1990**, *23*, 120-126.

[5] T. Friscic, W. Jones, *Journal of Pharmacy and Pharmacology* **2010**, *62*, 1547-1559.

[6] G. Bolla, A. Nangia, *Chemical Communications* **2016**, *52*, 8342-8360.

[7] D. Braga, F. Grepioni, L. Maini, *Chemical Communications* **2010**, *46*, 6232-6242.

[8] S. L. Childs, G. P. Stahly, A. Park, *Molecular Pharmaceutics* **2007**, *4*, 323-338.

[9] S. Aitipamula, R. Banerjee, A. K. Bansal, K. Biradha, M. L. Cheney, A. R. Choudhury, G. R. Desiraju, A. G. Dikundwar, R. Dubey, N. Duggirala, P. P. Ghogale, S. Ghosh, P. K. Goswami, N. R. Goud, R. Jetti, P. Karpinski, P. Kaushik, D. Kumar, V. Kumar, B. Moulton, A. Mukherjee, G. Mukherjee, A. S. Myerson, V. Puri, A. Ramanan, T. Rajamannar, C. M. Reddy, N. Rodriguez-Hornedo, R. D. Rogers, T. N. G. Row, P. Sanphui, N. Shan, G. Shete, A. Singh, C. Q. C. Sun, J. A. Swift, R. Thaimattam, T. S. Thakur, R. K. Thaper, S. P. Thomas, S. Tothadi, V. R. Vangala, N. Variankaval, P. Vishweshwar, D. R. Weyna, M. J. Zaworotko, *Crystal Growth & Design* **2012**, *12*, 2147-2152.

[10] T. Friscic, W. Jones, *Journal of Pharmacy and Pharmacology* **2010**, *62*, 1547-1559.

[11] U. S. F. a. D. Administration, **2016**, p. Draft.

[12] D. Braga, F. Grepioni, L. Maini, S. Prosperi, R. Gobetto, M. R. Chierotti, *Chemical Communications* **2010**, *46*, 7715-7717.

[13] D. Braga, L. Maini, F. Grepioni, *Chemical Society Reviews* **2013**, *42*, 7638-7648.

[14] S. Golob, M. Perry, M. Lusi, M. R. Chierotti, I. Grabnar, L. Lassiani, D. Voinovich, M. J. Zaworotko, *Journal of Pharmaceutical Sciences* **2016**, *105*, 3626-3633; A. R. Buist, A. R. Kennedy, *Crystal Growth & Design* **2014**, *14*, 6508-6513; N. K. Duggirala, A. J. Smith, L. Wojtas, R. D. Shytle, M. J. Zaworotko, *Crystal Growth & Design* **2014**, *14*, 6135-6142; J. Yao, J. M. Chen, Y. B. Xu, T. B. Lu, *Crystal Growth & Design* **2014**, *14*, 5019-5025; O. Shemchuk, D. Braga, L. Maini, F. Grepioni, *Crystengcomm* **2017**, *19*, 1366-1369.

[15] D. Braga, L. D. Esposti, K. Rubini, O. Shemchuk, F. Grepioni, *Crystal Growth & Design* **2016**, *16*, 7263-7270.

[16] L. D. Esposti, University of Bologna (Bologna, Italy), **2015-2016**.

[17] U. S. F. a. D. Administration, **1992**.

[18] A. Williams, *Pesticide Science* **1996**, *46*, 3-9.

[19] S. Srisanga, J. H. ter Horst, *Crystal Growth & Design* **2010**, *10*, 1808-1812.

[20] K. Busch, M. Busch *Chiral Analysis*, Elsevier Science, **2006**.

[21] A. A. Bredikhin, Z. A. Bredikhina, V. G. Novikova, A. V. Pashagin, D. V. Zakharychev, A. T. Gubaidullin, *Chirality* **2008**, *20*, 1092-1103; L. Perez-Garcia, D. B. Amabilino, *Chemical Society Reviews* **2007**, *36*, 941-967.

[22] T. Nishinaga, *Handbook of Crystal Growth Vol. VOLUME I, Part A* Second ed., Elsevier, **2015**.

[23] G. Springuel, K. Robeyns, B. Norberg, J. Wouters, T. Leyssens, *Crystal Growth & Design* **2014**, *14*, 3996-4004.

[24] S. L. James, C. J. Adams, C. Bolm, D. Braga, P. Collier, T. Friscic, F. Grepioni, K. D. M. Harris, G. Hyett, W. Jones, A. Krebs, J. Mack, L. Maini, A. G. Orpen, I. P. Parkin, W. C. Shearouse, J. W. Steed, D. C. Waddell, *Chemical Society Reviews* **2012**, *41*, 413-447.

[25] G. Springuel, T. Leyssens, *Crystal Growth & Design* **2012**, *12*, 3374-3378.

[26] F. George, B. Norberg, K. Robeyns, J. Wouters, T. Leyssens, *Crystal Growth & Design* **2016**, *16*, 5273-5282.
[27] C. Neurohr, M. Marchivie, S. Lecomte, Y. Cartigny, N. Couvrat, M. Sanselme, P. Subra-Paternault, *Crystal Growth & Design* **2015**, *15*, 4616-4626.
[28] G. A. Bowmaker, *Chemical Communications* **2013**, *49*, 334-348.
[29] K. Izutsu, T. Koide, N. Takata, Y. Ikeda, M. Ono, M. Inoue, T. Fukami, E. Yonemochi, *Chemical & Pharmaceutical Bulletin* **2016**, *64*, 1421-1430.
[30] D. Braga, F. Grepioni, *Chemical Communications* **2005**, 3635-3645.
[31] S. M. M. Pink, M. H. Baik, D. E. Clemmer, *Acta Crystallographica Section C-Crystal Structure Communications* **2005**, *61*, O506-O508.
[32] R. T. Berendt, E. J. Munson, *Crystengcomm* **2012**, *14*, 2479-2488.
[33] A. Tilborg, B. Norberg, J. Wouters, *European Journal of Medicinal Chemistry* **2014**, *74*, 411-426.
[34] A. J. Smith, S. H. Kim, N. K. Duggirala, J. Jin, L. Wojtas, J. Ehrhart, B. Giunta, J. Tan, M. J. Zaworotko, R. D. Shytle, *Molecular Pharmaceutics* **2013**, *10*, 4728-4738.
[35] M. Shkir, S. Alfaify, M. A. Khan, E. Dieguez, J. Perles, *Journal of Crystal Growth* **2014**, *391*, 104-110.
[36] S. Sathiskumar, T. Balakrishnan, K. Ramamurthi, S. Thamotharan, *Acta Crystallographica Section E-Crystallographic Communications* **2015**, *71*, 1199-+; T. U. Devi, N. Lawrence, R. R. Babu, S. Selvanayagam, H. Stoeckli-Evans, K. Ramamurthi, *Crystal Growth & Design* **2009**, *9*, 1370-1374; S. Sathiskumar, T. Balakrishnan, K. Ramamurthi, S. Thamotharan, *Spectrochimica Acta Part a-Molecular and Biomolecular Spectroscopy* **2015**, *138*, 187-194.
[37] M. Shkir, S. AlFaify, M. A. Khan, S. Muhammad, A. R. Chaudhry, *Optik* **2016**, *127*, 2852-2860; D. Kalaiselvi, R. Jayavel, *Optoelectronics and Advanced Materials-Rapid Communications* **2011**, *5*, 58-62.
[38] T. T. Ong, P. Kavuru, T. Nguyen, R. Cantwell, L. Wojtas, M. J. Zaworotko, *Journal of the American Chemical Society* **2011**, *133*, 9224-9227.
[39] D. Anbuselvi, D. Jayaraman, J. A. M. Mani, V. Joseph, *Spectrochimica Acta Part a-Molecular and Biomolecular Spectroscopy* **2014**, *127*, 405-414; G. A. Babu, P. Ramasamy, *Materials Chemistry and Physics* **2009**, *113*, 727-733; U. Charoen-In, P. Ramasamy, P. Manyum, *Journal of Crystal Growth* **2013**, *362*, 220-226; M. Shkir, V. K. Jain, S. AlFaify, M. M. Abutalib, I. S. Yahiya, M. A. Khan, *Journal of Theoretical & Computational Chemistry* **2015**, *14*, 20; Y. Yukawa, N. Yasukawa, Y. Inomata, T. Takeuchi, *Bulletin of the Chemical Society of Japan* **1985**, *58*, 1591-1592.
[40] M. Lutz, R. Bakker, *Acta Crystallographica Section C-Crystal Structure Communications* **2003**, *59*, M18-M20.
[41] K. Lamberts, S. Porsche, B. Hentschel, T. Kuhlen, U. Englert, *Crystengcomm* **2014**, *16*, 3305-3311.
[42] G. Sheldrick University of Göttingen, Germany, **1997**.
[43] C. F. Macrae, I. J. Bruno, J. A. Chisholm, P. R. Edgington, P. McCabe, E. Pidcock, L. Rodriguez-Monge, R. Taylor, J. van de Streek, P. A. Wood, *Journal of Applied Crystallography* **2008**, *41*, 466-470; I. J. Bruno, J. C. Cole, P. R. Edgington, M. Kessler, C. F. Macrae, P. McCabe, J. Pearson, R. Taylor, *Acta Crystallographica Section B-Structural Science* **2002**, *58*, 389-397; C. F. Macrae, P. R. Edgington, P. McCabe, E. Pidcock, G. P. Shields, R. Taylor, M. Towler, J. van De Streek, *Journal of Applied Crystallography* **2006**, *39*, 453-457.
[44] K. Momma, F. Izumi, *Journal of Applied Crystallography* **2011**, *44*, 1272-1276.
[45] Bruker Analytical Systems, Madison, WIsconsin, **2005**.
[46] T. Degen, M. Sadki, E. Bron, U. Konig, G. Nenert, *Powder Diffraction* **2014**, *29*, S13-S18.
[47] A. Altomare, C. Cuocci, C. Giacovazzo, A. Moliterni, R. Rizzi, N. Corriero, A. Falcicchio, *Journal of Applied Crystallography* **2013**, *46*, 1231-1235.
[48] A. Cohelo, Coelho Software, Brisbane,Australia, **2007**.

[49] C. P. Brock, W. B. Schweizer, J. D. Dunitz, *Journal of the American Chemical Society* **1991**, *113*, 9811-9820.
[50] H. G. Brittain*, Vol. 162*, Second ed., Informa Healthcare USA, Inc., **2009**.
[51] S. Aitipamula, P. S. Chow, R. B. H. Tan, *Crystengcomm* **2014**, *16*, 3451-3465; M. J. Bevill, P. I. Vlahova, J. P. Smit, *Crystal Growth & Design* **2014**, *14*, 1438-1448; G. Bolla, S. Mittapalli, A. Nangia, *Crystengcomm* **2014**, *16*, 24-27; F. Fischer, G. Scholz, S. Benemann, K. Rademann, F. Emmerling, *Crystengcomm* **2014**, *16*, 8272-8278; F. Fischer, A. Heidrich, S. Greiser, S. Benemann, K. Rademann, F. Emmerling, *Crystal Growth & Design* **2016**, *16*, 1701-1707; H. Kulla, S. Greiser, S. Benemann, K. Rademann, F. Emmerlingt, *Crystal Growth & Design* **2017**, *17*, 1190-1196; J. B. Nanubolu, K. Ravikumar, *Crystengcomm* **2017**, *19*, 355-366; A. Sokal, E. Pindelska, L. Szeleszczuk, W. Kolodziejski, *International Journal of Pharmaceutics* **2017**, *522*, 80-89; A. O. Surov, A. N. Manin, A. P. Voronin, A. V. Churakov, G. L. Perlovich, M. V. Vener, *Crystal Growth & Design* **2017**, *17*, 1425-1437.
[52] C. Butterhof, K. Barwinkel, J. Senker, J. Breu, *Crystengcomm* **2012**, *14*, 6744-6749.

ANNEXES

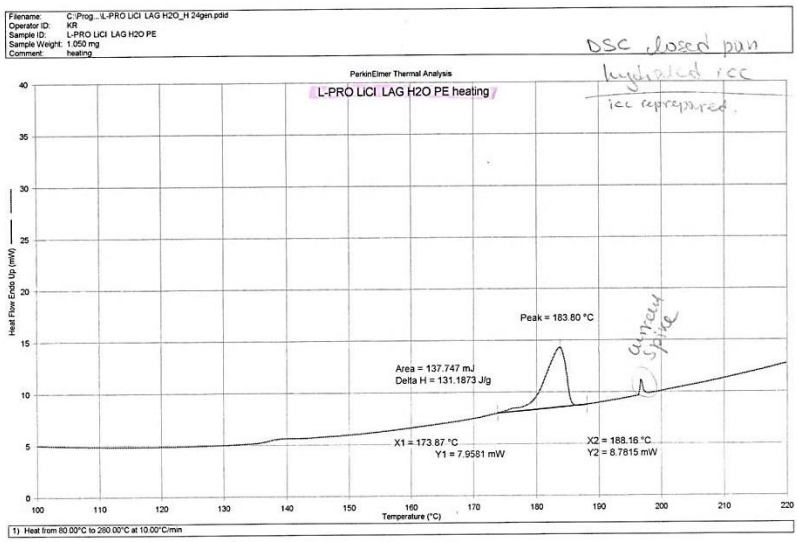

Figure 1: DSC Analysis of L-Pro•LiCl•H_2O performed in a closed pan.

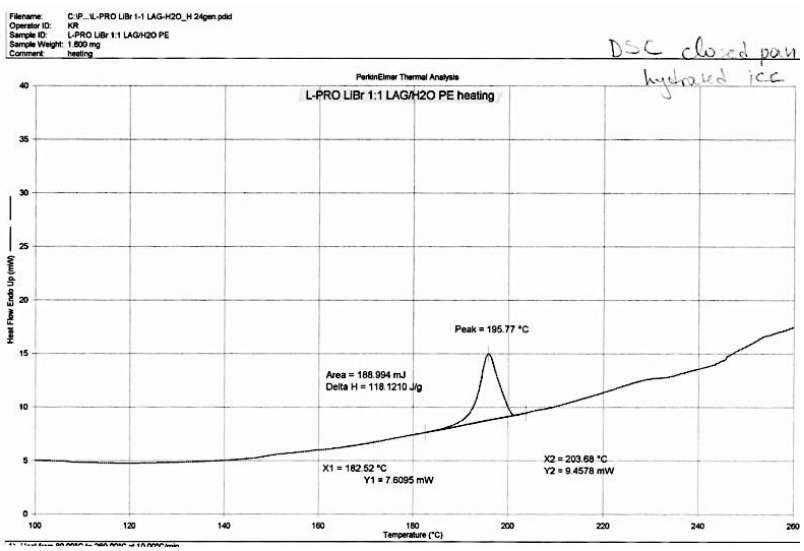

Figure 2: DSC Analysis of L-Pro•LiBr•H_2O performed in a closed pan.

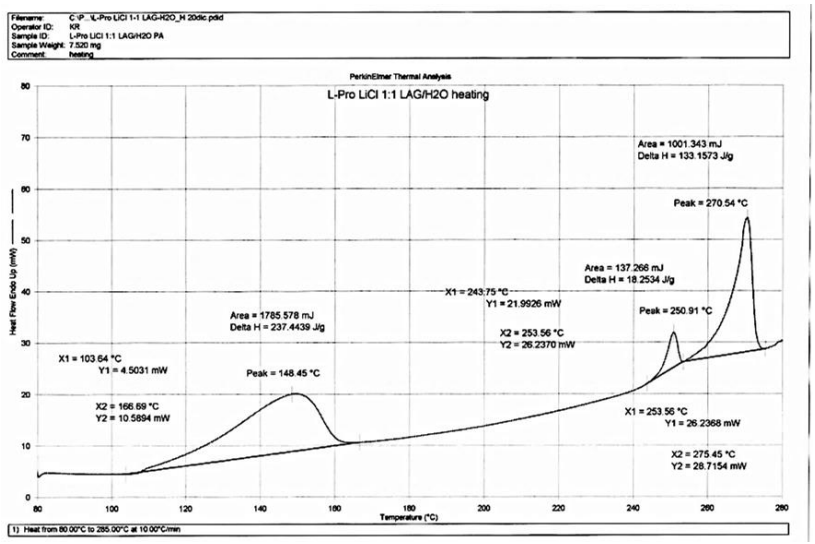

Figure 3: DSC Analysis of L-Pro•LiCl•H_2O performed in an open pan.

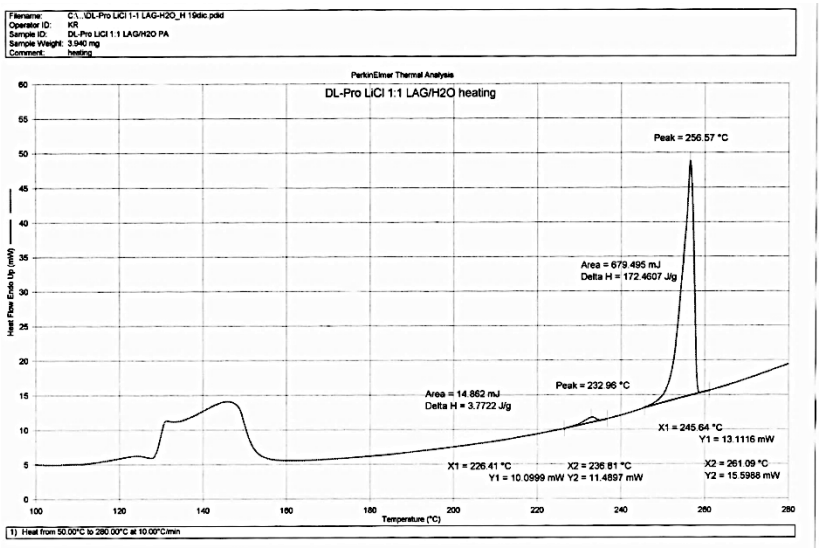

Figure 4: DSC Analysis of DL-Pro•LiCl•H_2O performed in an open pan.

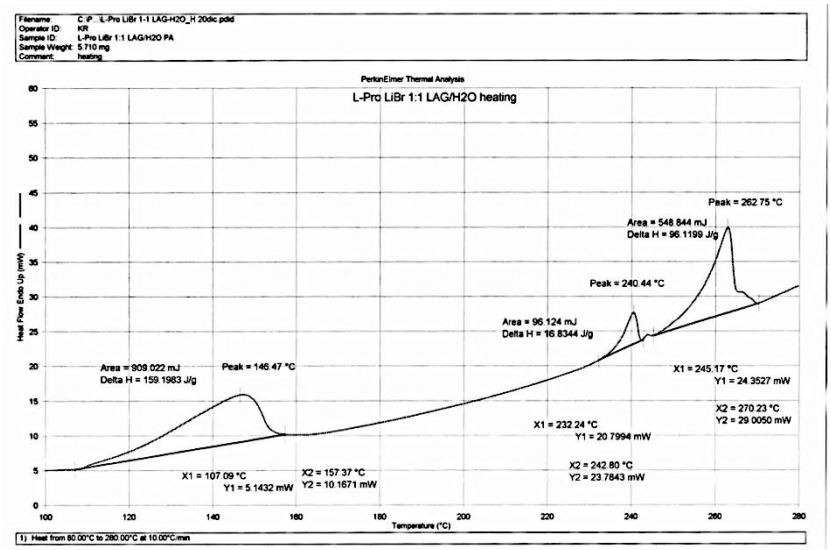

Figure 5: DSC Analysis of L-Pro•LiBr•H_2O performed in an open pan.

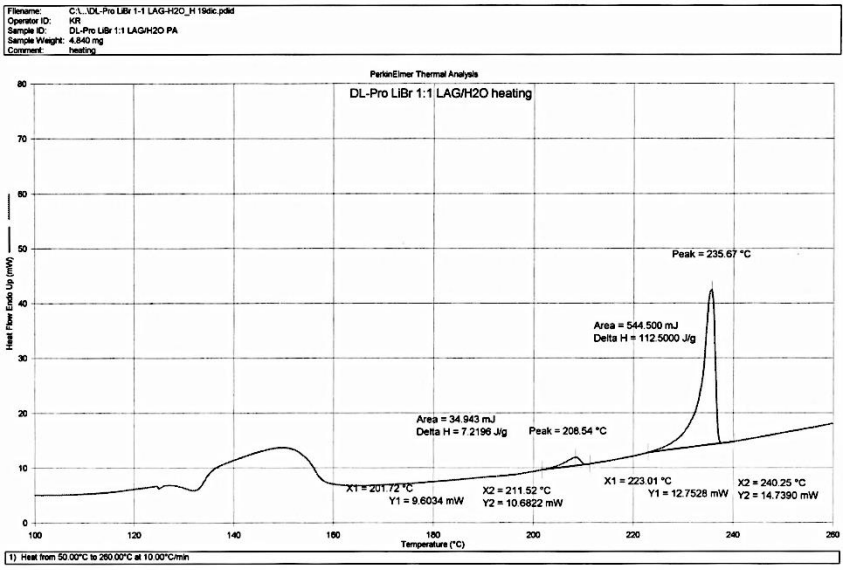

Figure 6: DSC Analysis of DL-Pro•LiBr•H_2O performed in an open pan.

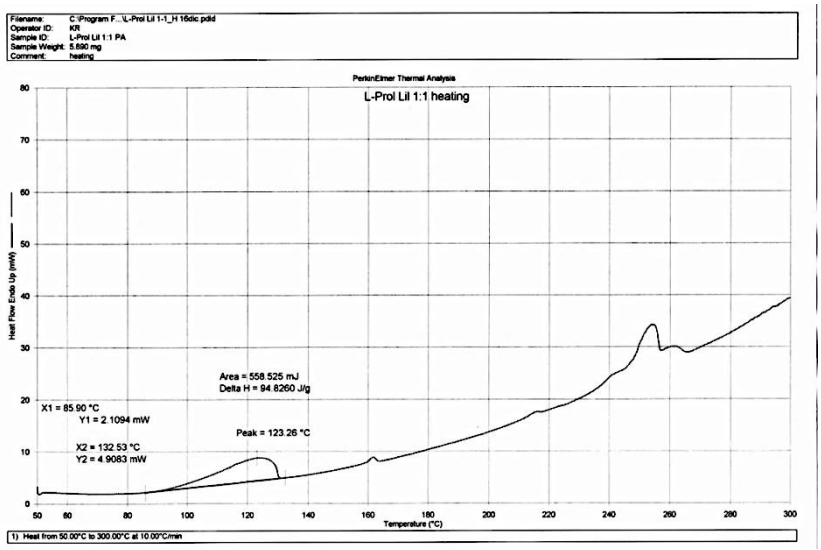

Figure 7: DSC Analysis of L-Pro•LiI•H_2O performed in an open pan.

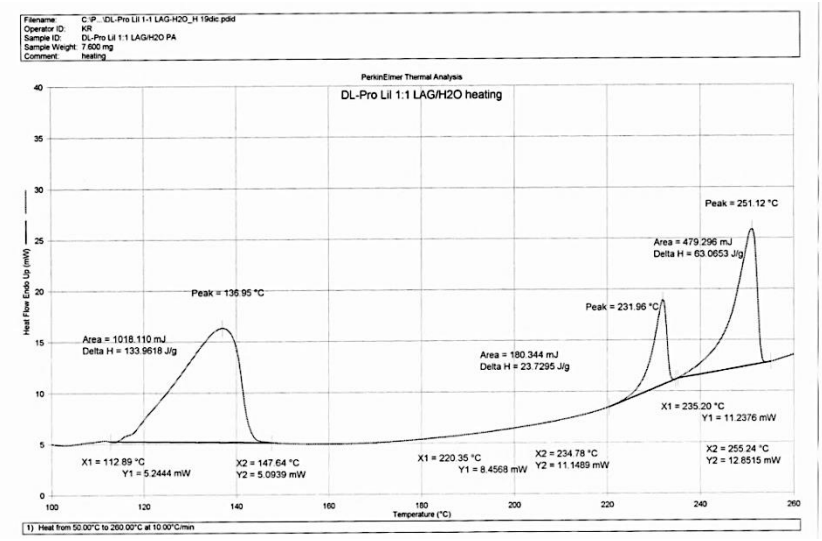

Figure 8: DSC Analysis of DL-Pro•LiI•H_2O performed in an open pan.

Table 1: Anhydrous structures solved from powder.

ICC	R_wp	COMMENTS
L-Pro•LiCl	7.89%	There are peaks of CCDC:EVUVUN which are well described by Topas.
DL-Pro•LiCl	12.15%	Huge R_wp value due to the presence of the unidentified phase. However, the XRPD patterns are very similar which supports the correctness of this structure solution.
L-Pro•LiBr	4.55%	There are peaks of CCDC:EVUVIB which are well described by Topas.
DL-Pro•LiBr	6.26%	Similar to LiCl but there is an unidentified phase

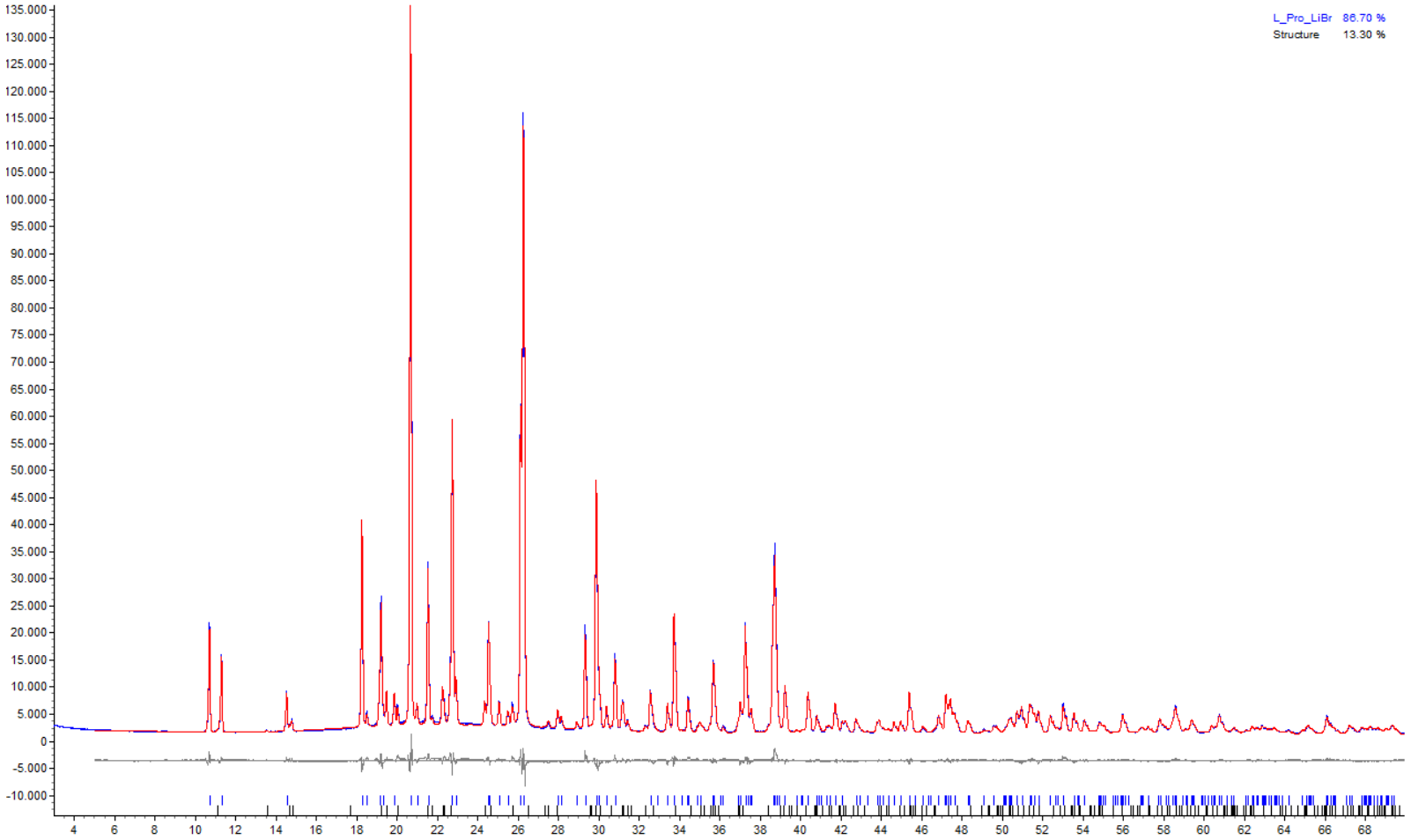

Figure 9: Rietveld analysis plot of L-Pro•LiCl. Red line is the calculated diffractogram, blue line is the observed diffractogram and grey line is the difference plot. Blue and black tick marks correspond to L-Pro•LiCl and CCDC: EVUVUN respectively. Y-axis is reported as $\sqrt{y}$.

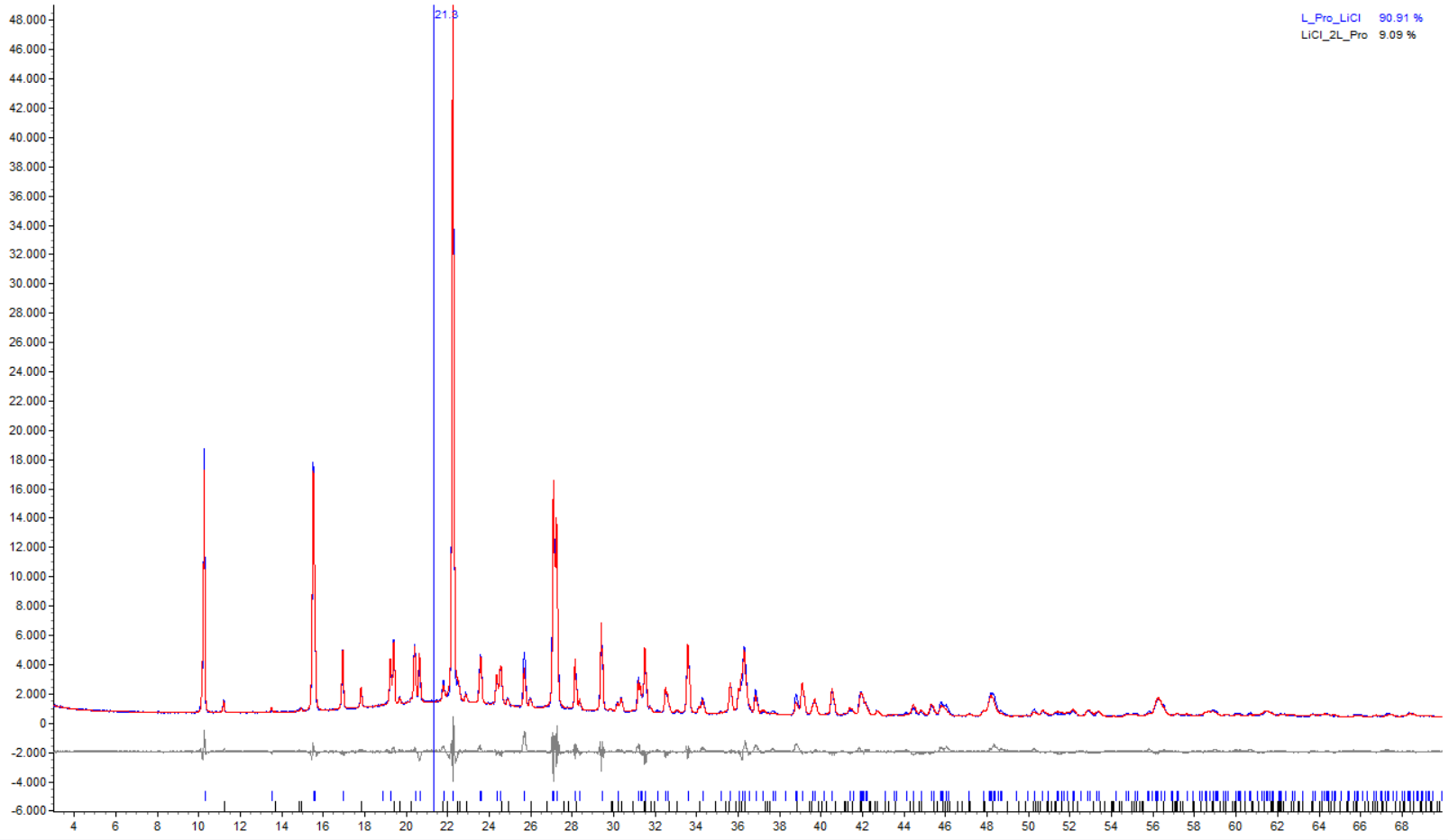

Figure 10: Rietveld analysis plot of L-Pro•LiBr. Red line is the calculated diffractogram, blue line is the observed diffractogram and grey line is the difference plot. Blue and black tick marks correspond to L-Pro•LiBr and CCDC: EVUVIB respectively. Y-axis is reported as $\sqrt{y}$.

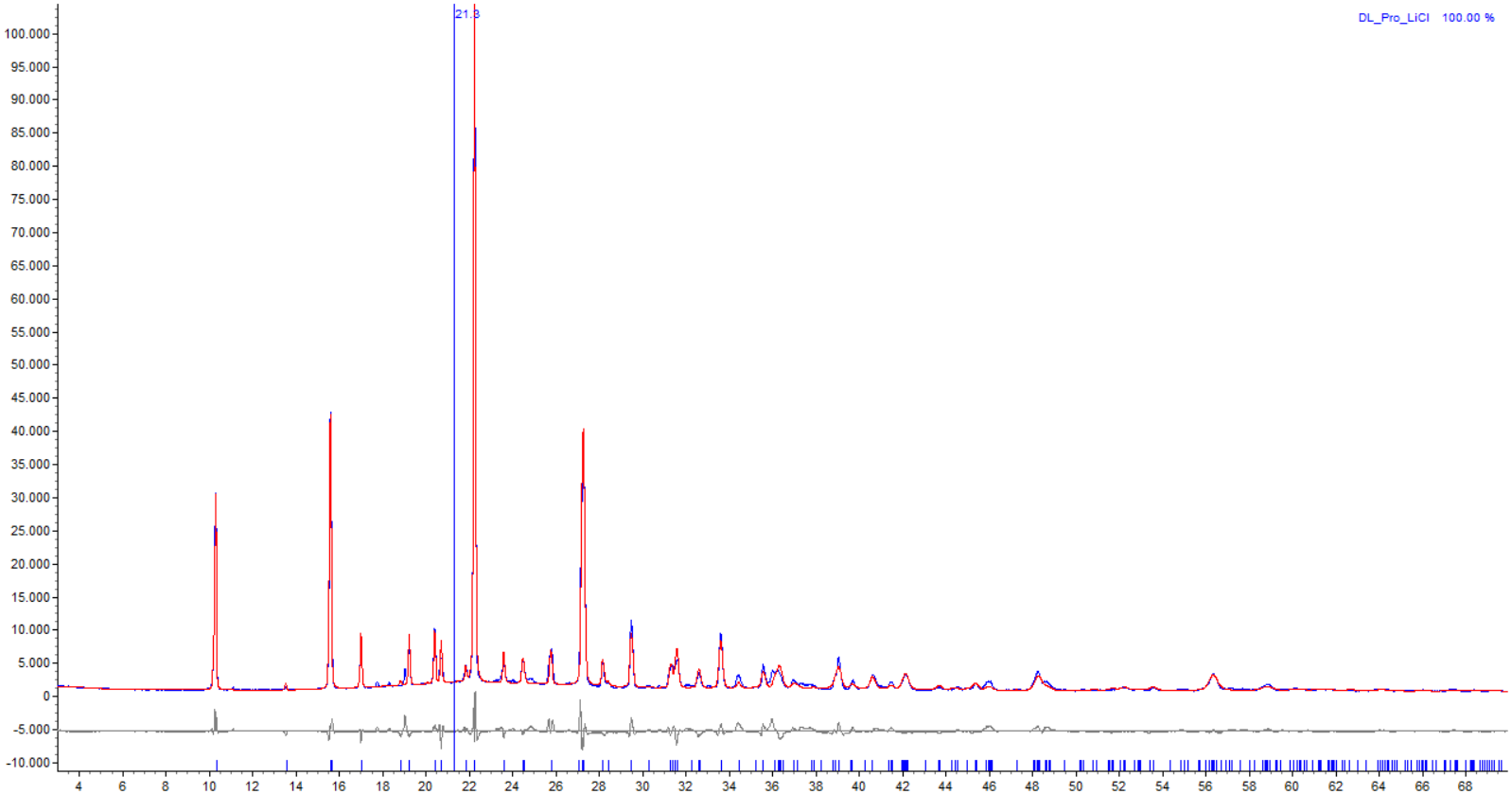

Figure 11: Rietveld analysis plot of DL-Pro•LiCl. Red line is the calculated diffractogram, blue line is the observed diffractogram and grey line is the difference plot. Blue tick marks corresponds to L-Pro•LiCl. Y-axis is reported as $\sqrt{y}$.

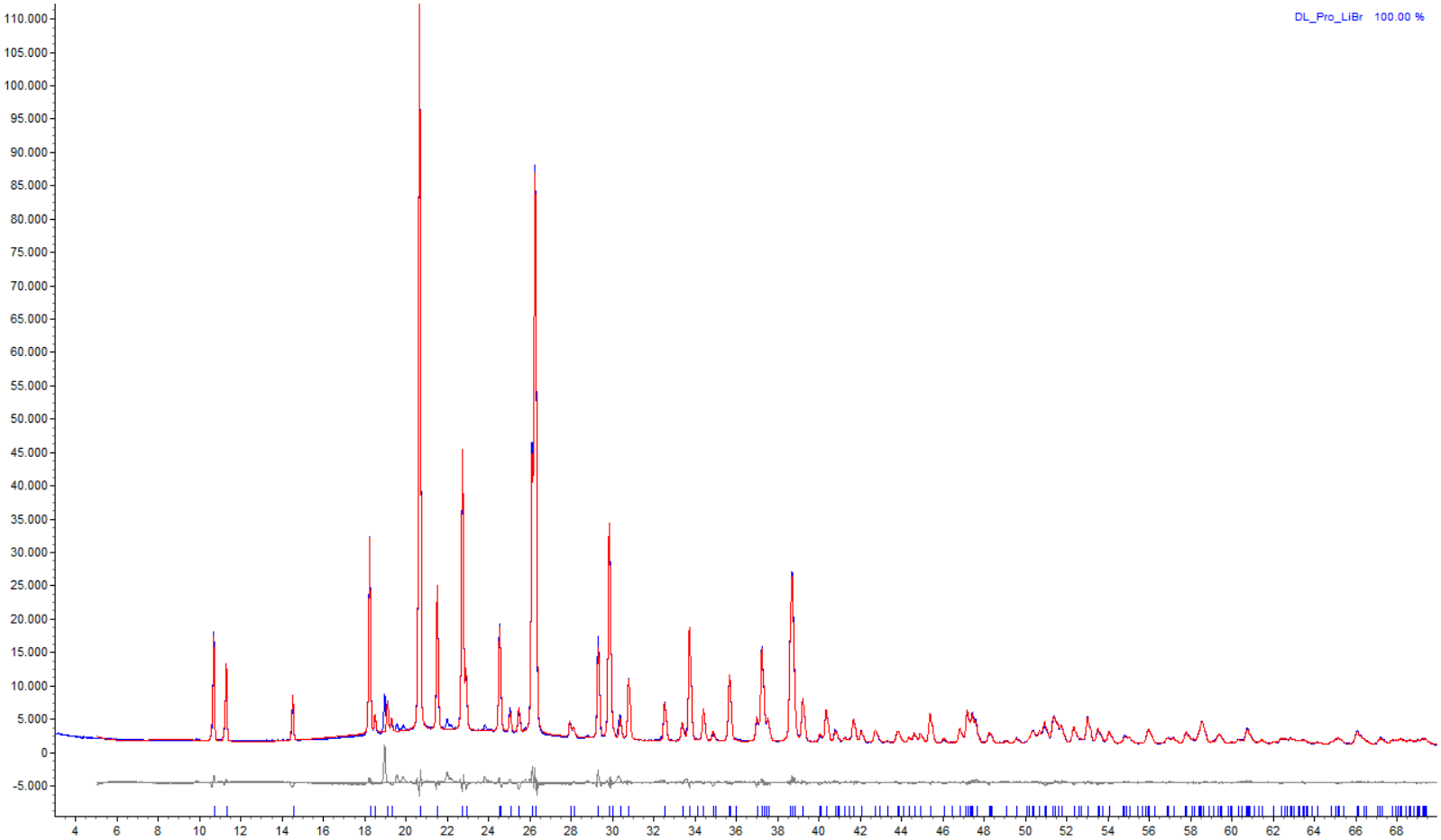

Figure 12: Rietveld analysis plot of DL-Pro•LiBr. Red line is the calculated diffractogram, blue line is the observed diffractogram and grey line is the difference plot. Blue tick marks corresponds to L-Pro•LiBr. Y-axis is reported as $\sqrt{y}$.